

Production of geopolymers from diatomaceous earth for wastewater treatment

Alia Balkiss Chalghmi

Thesis report presented to

Escola Superior de Tecnologia e Gestão

Instituto Politécnico de Bragança

to obtain a master's degree in

Chemical Engineering

within the scope of the double diploma with

Université libre de Tunis

Supervisors:

Prof. Helder Teixeira Gomes

Prof. Khalil Zaghdoudi

Dr. Jose Luis Díaz de Tuesta Triviño

Bragança

2022

ACKNOWLEDGEMENTS

As with any piece of research the results in the production of a thesis, on the cover there should be not only the name of the researcher, but also the names of all unsung heroes, those who to varying degrees provided assistance, guidance, and without whom I would not have succeeded. I am very grateful to all those people, my heroes, who have given me so much of their time, love, energy. In producing this thesis, I faced a key step in my academic challenge, to gain a master's degree.

There are so many people that I would like to thank, first, I would like to thank my supervisors at Instituto Politécnico de Braganca (IPB), Professor Helder Teixeira Gomes and Dr. Jose Luis Diaz de Tuesta Triviño, and my supervisor at Université Libre de Tunis (ULT) Professor Khalil Zaghdoudi, for their help and support throughout this process. Secondly, I must thank IPB for allowing me with an Erasmus grant and ULT for giving me this opportunity to be a part of double diploma program. Finally, without the support and love of my family and friends I know I could never have accomplished this thesis.

This work is a part of the project BacchusTech of CIMO.



ABSTRACT

Geopolymers (GPs) are inorganic binders created by adding an alkaline solution (e.g., NaOH) to silicates, such as furnace slags, fly ashes or clays, to dissolve Si and Al that polymerizes and precipitates to form an inorganic binder material while hardening. GP properties are similar to ordinary Portland cement, since it presents high compressive strength or low shrinkage, but they are particularly notable for a high resistance to acid and fire. For this reason, GP has been widely studied in its application in civil engineering. However, GPs presents other interesting properties that make it an excellent material to be used as adsorbent.

The aim of this study is to investigate the suitability of commercial diatomaceous earth as a cheaper alternative to kaolin and to determine the necessary preparation steps required to produce effective geopolymer adsorbent materials. Geopolymerization is a multi-parameter system strongly influenced by the degree of activation, Si:Al ratio, amount of 5-fold coordinated Al and curing mode. Bearing this in mind, different formulations to yield geopolymeric solid samples were examined. Important parameters for the production, such as temperature, time, and heating rate are determined and discussed. Additionally, geopolymers were assessed in the removal of gallic acid and phenol, used as model pollutants, from aqueous solutions by adsorption.

The results presented in this thesis indicate that commercial diatomaceous earth is a suitable raw material for geopolymer production. Proxies used to evaluate the optimal conditions for making geopolymers are determined including the Si/Al ratio as a key relationship that determines its ultimate hardness and curing mode as key factor that controls the geopolymerization process.

KEYWORDS: geopolymer synthesis, chemical activation, diatomaceous earth, wastewater treatment, valorisation technologies.

RESUMO

Os geopolímeros (GPs) são ligantes inorgânicos criados pela adição de uma solução alcalina (por exemplo NaOH) aos silicatos, tais como escórias do forno, cinzas volantes ou argilas, para dissolver o Si e o Al que polimeriza e precipita para formar um material aglutinante inorgânico enquanto endurece. As propriedades do GP são semelhantes ao cimento Portland comum no que diz respeito à sua alta resistência à compressão ou baixa retracção, mas são particularmente notáveis para uma alta resistência ao ácido e ao fogo. Além disso, os geopolímeros podem ser utilizados como adsorventes de poluentes da água.

As matérias-primas mais comuns utilizadas na produção de GPs são argilas de caulino. Assim, o objectivo deste estudo é investigar a adequação da terra de diatomáceas comerciais como uma alternativa mais barata ao caulino e determinar as etapas de preparação necessárias para produzir materiais adsorventes de geopolímeros eficazes. Foram examinadas diferentes formulações para produzir amostras sólidas geopoliméricas. Foram determinados e discutidos parâmetros importantes para a produção, tais como temperatura, tempo, e taxa de aquecimento.

A geopolimerização é um sistema multi-parâmetros fortemente influenciado pelo grau de activação, razão Si:Al, quantidade de Al coordenada em 5 vezes e modo de cura. Os resultados apresentados nesta tese indicam que a terra diatomácea comercial é uma matéria prima adequada para a produção de geopolímeros. Os proxies utilizados para avaliar as condições óptimas para a produção de geopolímeros são determinados incluindo a relação Si/Al como uma relação chave que determina a sua dureza final e o modo de cura como factor chave que controla o processo de geopolimerização.

PALAVRAS-CHAVE: síntese de geopolímeros, activação química, terra de diatomáceas, tratamento de águas residuais, valorização.

TABLE OF CONTENTS

INDEX OF TABLES	viii
LIST OF ABBREVIATIONS	ix
I. INTRODUCTION	2
II. STATE OF THE ART.....	5
II.1 DIATOMACEOUS EARTH: WASTE SOURCE	5
II.2 GEOPOLYMERS.....	6
II.2.1 HISTORY	6
II.2.2 CHEMICAL STRUCTURE.....	9
II.2.3 PROPERTIES	9
II.2.4 GEOPOLYMER APPLICATIONS	10
II.3 PRODUCTION	10
II.3.1 GEOPOLYMERIZATION PROCESS.....	11
II.3.2 RAW MATERIAL.....	16
II.3.3 ACTIVATING SOLUTIONS AND TYPICAL CONDITIONS.....	20
II.4 ADSORBENT CHARACTER OF GEOPOLYMERS FOR WATER TREATMENT.....	23
II.4.1 ADSORPTION KINETICS	28
II.4.2 ADSORPTION ISOTHERMS AND MECHANISMS	30
III. METHODOLOGY	32
III.1 REACTANTS	32
III.2 GEOPOLYMER'S PREPARATION	32
III.3 CHARACTERIZATION OF GEOPOLYMERS	35
III.3.1 CHARACTERISATION OF THE GEOPOLYMER AS POWDER MATERIAL :	35
III.3.2 APPLICATION OF GEOPOLYMER AS ADSORBENT IN POWDER FORM	35

IV.	RESULTS AND DISCUSSION	40
IV.1	APPEARANCE OF THE GEOPOLYMERS.....	40
IV.2	pH EVOLUTION IN GEOPOLYMERS WASHING.....	42
IV.3	CHARACTERIZATION OF THE SELECTED GEOPOLYMER.....	44
IV.4	APPLICATION RESULTS OF THE GEOPOLYMER SAMPLE AS ADSORBENT IN POWDER FORM	45
IV.4.1	PRELIMINARY TEST RESULTS	45
IV.4.2	ADSORPTION ISOTHERMS	47
V.	CONCLUSIONS AND OUTLOOKS:.....	51
VI.	REFERENCES	53
VII.	APPENDIX	58

INDEX OF FIGURES

Figure 1- Evolution of the research scope, approximate timeline and notable mentions; adaptation from source	8
Figure 2 - Synthesis stages of geopolymers; adaptation from source	12
Figure 3 - Si-O-Si bond breakage mechanism by the reaction of OH ⁻ ions; adaptation from source.....	13
Figure 4 - Chemical equation of geopolymers synthesis; adaptation from source.....	14
Figure 5 - Conceptual model of geopolymerization; adaptation from source	15
Figure 6 - Main factors influencing preparation of geopolymers; adaptation from source	16
Figure 7 - Categories of waste sources that can be used as a precursor of geopolymers; adaptation from source	17
Figure 8 - Difference between cements, alkali activated materials and geopolymers according to their composition; adaptation from source	20
Figure 9 - Example of a geopolymer sample (a) during and (b) after stirring.	34
Figure 10 - Phenol calibration curve by UV/Vis spectrophotometry using a wavelength of 270 nm.	36
Figure 11 - Gallic acid calibration curve by UV/Vis spectrophotometry using a wavelength of 260 nm.	36
Figure 12 - Agitation of the geopolymer samples in adsorbate solutions in the orbital shaker	37
Figure 13 - Samples 21-26 before curing process.	41
Figure 14 - Samples 21-26 after 2 days in wet chamber and 3 days in oven.	42
Figure 15 – pH evolution of the rising water during washing geopolymers.	43
Figure 16 - Geopolymer sample after drying.	43
Figure 17 - Non-washed geopolymer sample 15 placed in distilled water for a day. ...	44

Figure 18 - FT-IR spectrum of the geopolymer sample 15 after washing and drying.	44
Figure 19 - FT-IR spectrum of geopolymer sample after the gallic acid adsorption test.	46
Figure 20 - FT-IR spectrum of the geopolymer sample after the phenol adsorption test.	47
Figure 21 - Isotherm of gallic acid adsorption.	48
Figure 22 - Isotherm of phenol adsorption	49
Figure 23 - Isotherm curve shape	49

INDEX OF TABLES

Table 1 - Composition of 2 examples of wasted diatomaceous earth	6
Table 2 - Calculated energy for different condensation reactions.....	11
Table 3 - Synthesis experiences of geopolymers using diatomaceous earth.....	18
Table 4 - Previous studies on the adsorption of dyes and heavy metals with geopolymers	25
Table 5 : Kinetics and isotherm studies of the adsorption of dyes and heavy metals with geopolymers based on different raw materials.....	29
Table 6 - Formulas used to produce geopolymer samples.	33
Table 7 - Equilibrium concentration of the adsorbate in solution (C_e), equilibrium uptake capacity (q_e) and Removal (R) obtained in the adsorption of gallic acid and phenol on the geopolymer.....	45
Table 8 - Isotherm data for gallic acid adsorption.....	47
Table 9 - Isotherm data for phenol adsorption	48

LIST OF ABBREVIATIONS

- AAM – Alkaline activated materials;
- AAC – Alkaline activated cement;
- GPC – Geopolymer concrete;
- OPC – Ordinary Portland concrete;
- ISO – International Organization for Standardization;
- IPPC – Integrated pollution prevention and control;
- GFC – Geopolymer foam concrete;
- FTIR – Fourier transform infrared spectroscopy.

INTRODUCTION

I. INTRODUCTION

The discovery of a new class of inorganic materials, geopolymers, attracted a wide scientific interest and initiated kaleidoscopic development of applications. Since the first industrial research experiences in 1972 at the Cordi-Géopolymère private research laboratory, Saint-Quentin, France, till 2021, thousands of papers and patents have been published discussing geopolymer science and technology. On August 31, 2005, a non-profit scientific organization founded in 1979, the Geopolymer Institute, announced: "Since 1997, 80000 papers have been downloaded by 15000 scientists around the world at the geopolymer.org website"[1].

Several major conferences have proved the degree of international scientific and commercial interest in geopolymers. The first European Conference on Soft Mineral Compounds was held at the Compiègne University of Technology in France in June 1988 (Geopolymer`88), organized by the Geopolymer Institute and under the auspices of the European Economic Commission. The Geopolymer Institute organized the Second International Conference Geopolymere'99 in Saint-Quentin eleven years later, in June-July 1999; the published proceedings covered 32 papers presented to 100 scientists from over 12 countries. In October 2002, the Third International Conference, Geopolymer 2002, took place in Melbourne, Australia. Many national and international scientific institutions have organized geopolymer conferences, seminars and sessions since 2003 [1].

The 26th anniversary of the Geopolymer institute's creation by Davidovits marked the occasion of the 2005 World Congress. Geopolymer-chemistry and sustainable development were the main topics of the congress. It gathered two major events in two different locations: the Fourth International Conference in Saint-Quentin, France, June-July 2005, organized by the Geopolymer Institute; and the International Workshop on Geopolymer Cements and Concrete in Perth, Australia, September 2005, organized by V.J. Rangan of Curtin University of Technology, Perth, the University of Alabama, USA, and sponsored by the National Science Foundation, USA. Over 200 scientists attended the congress, and 85 international public and private research institutions presented 75 papers. They cover topics ranging from geopolymer chemistry, industrial wastes, raw materials, geopolymer cement, geopolymer concretes (including fly ash-based geopolymers), applications to construction materials, applications in high-tech materials, matrix for fire/heat resistant composites and applications to archeology. Published proceedings (Geopolymer 2005) consist of 60 selected papers titled: Geopolymer, Green Chemistry and Sustainable Development Solutions [1].

Geopolymers are ceramic-like inorganic polymers synthesized at low temperatures (generally $< 100^{\circ}\text{C}$). They are chains or 3D networks of mineral molecules with covalent bonds linking. New materials for coatings and adhesives, new binders for fiber composites, waste encapsulation, and new cement for concrete have been developed based on geopolymers. Researchers are exploring the properties and uses of geopolymers in many fields of science and industry, including modern inorganic chemistry, physical chemistry, mineralogy, colloid chemistry, geology, and all engineering process technologies. Among the wide range of potential applications can be named the following: fire-resistant materials, thermal insulation, decorative stone artifacts, low-energy ceramic tiles, low-tech building materials, refractory items, thermal shock refractories, foundry industry, biotechnologies (for medicinal applications), cement and concretes, high-tech composites for aircraft interior and automobile, composites for infrastructure repair and strengthening, high-tech resin systems and radioactive materials. Geopolymer materials can effectively adsorb heavy metals, dyes and other radioactive pollution, which benefits society's water treatment process development. Geopolymers are proven susceptible to being synthesized from waste solids such as wasted diatomaceous earth, fly ash and sludge [1].

This thesis subject comes as part of an ongoing project of Centro de Investigação de Montanha (Mountain Research Center), which involves the valorization of winemaking waste of a Portuguese winery. The objective of this thesis is to study the feasibility of transforming a part of this waste which is wasted diatomaceous earth into a geopolymer material that can be used as adsorbent of gallic acid and phenol for wastewater treatment of a wine industry. To this aim, it is proposed to produce geopolymers from commercial diatomaceous earth combined with an aluminum source as raw materials with activating solutions based on sodium hydroxide and liquid glass. In the dissertation work that follows, a state of the art is presented in the second chapter, a methodology is detailed in the third chapter, then the results and discussion of the experimental work is presented in the fourth chapter, finally the conclusions and outlooks chapter followed by the references and appendix.

STATE OF THE ART

II. STATE OF THE ART

II.1 DIATOMACEOUS EARTH: WASTE SOURCE

Wine is an integral part of Portuguese cultural heritage and economy, the wine sector is considered one of the most dynamic Portuguese agricultural exports. Environmentally and economically sustainable winery waste management should be a priority for the industry. The main environmental affection associated with wineries includes soil degradation, water pollution, damage to vegetation, odors and air emissions. The wine sector, like others, needs to minimize its environmental impact, allowing the reduction of water consumption, the recovery of by-products and the reduction of waste, as foreseen in ISO 14000, which includes a series of standards; ISO 14001 addresses different aspects of environmental management and pollution prevention, providing fundamental principles for implementing an Environmental Management System and reducing environmental risks. The IPPC Directive 2008/1/EC also fosters the application of best techniques and environmental practices as it ensures a high level of environmental protection, balancing the costs to the operator and the benefits to the environment [2].

There are five basic stages to produce wine: harvesting, crushing and pressing, fermentation, clarification (filtration) and finally, aging and bottling. Diatomaceous earth, also known as diatomite and DE, is one of the clarification methods used for wine. The pores within and between the cell walls of diatomaceous earth are so small, being able to trap bacteria, clay particles, some viruses and other suspended solids from liquids. This makes the wine cleaner, drastically reducing solids and lowering contamination level [3]. On the other hand, there's waste of big amounts of exhausted diatomaceous earth that needs to be treated or valorized.

Diatomite is a sedimentary rock attributable to siliceous fossilized skeletons of diatoms that are single-celled (unicellular) organisms that produce intricately formed cytoskeletons constructed from silica. When diatoms die, their silica husks accumulate on the seafloor, and thick layers of these diatom husks are fossilized into diatomaceous earth or diatomite. Diatomaceous earth, a rich and inexpensive mineral, is essentially $(\text{SiO}_2 \cdot n\text{H}_2\text{O})$ where n varies from 0.5 to 4 depending on the type and contains large amounts of amorphous hydrated or opaline silica, giving it a microporous structure. Diatomaceous earth is widely used as a thermal insulator in manufacturing porous ceramic functional filters, paint bulking agents, ceramic forming precursors, such as SiC , Si_3N_4 , and absorbent materials. It presents an average specific surface area (can exceed 5 to 200 m^2/g), low bulk density and high absorption capacity. Finally,

diatomaceous earth is used as an alternative to fly ash and as an additive for alkali-activated fly ash-based cement. In addition, it is used in the manufacturing of lightweight concrete and industrial geopolymers and as a cement additive in various compositions [4].

After usage as a filter in the winery and beer industry, diatomaceous earth accumulates some components to have a final composition like in examples shown in Table 1.

Table 1 - Composition of 2 examples of wasted diatomaceous earth

	SiO ₂	Al ₂ O ₃	Fe ₂ O ₃	CaO	MgO	SO ₃	K ₂ O	Na ₂ O	P ₂ O ₅	TiO ₂	LOI
BD	81.7	5.67	3.71	1.28	0.41	-	0.86	1.3	0.36	0.93	3.34
WD	71.89	6.95	1.77	1.2	0.26	1.89	2.58	1.33	-	0.45	11.05

BD: exhausted diatomaceous earth from beer filtration supplied by Heineken (Quart de Poblet, Spain).

WD: exhausted diatomaceous earth from wine filtration supplied by Bodegas Vicente Gandia (Utiel, Spain) [5].

According to the examples given in Table 1, waste diatomaceous earth is rich in aluminates and silicates, presenting potential to be used as raw material for synthesis of geopolymers.

II.2 GEOPOLYMERS

High-temperature techniques are no longer necessary to obtain hard and chemically non-reactive materials since 1978. In fact, geopolymers are inorganic polymers that are ceramic-like in their structures and properties, and that can be synthesized at ambient temperature [6]. Distinguished by their fuel efficiency, they are gaining more and more attraction in interdisciplinary research [4]. Indeed, in 2021, the global geopolymer market was valued at US\$ 5 billion, and according to IMARC Group, the market would reach US\$ 15.8 billion by 2027, with a compound annual growth rate of 21.5 percent from 2022 to 2027 [7].

Regarding the name "geopolymer", "geo" indicates its derivation from geological materials and "polymer" refers to the macromolecular structure formed by mixing an aluminosilicate source with an alkaline meta-silicate solution at ambient temperature.

II.2.1 HISTORY

The term 'geopolymer' was coined by the French scientist and engineer Professor Joseph Davidovits in the 1970s and refers to a class of solid materials synthesized by an aluminosilicate powder with an alkaline solution. These materials were originally developed as a fire-resistant

alternative to organic thermosetting polymers following a series of fires happened in European [8].

Fig.1 represents the different research axis evolution associated with geopolymers since 2010 [9].

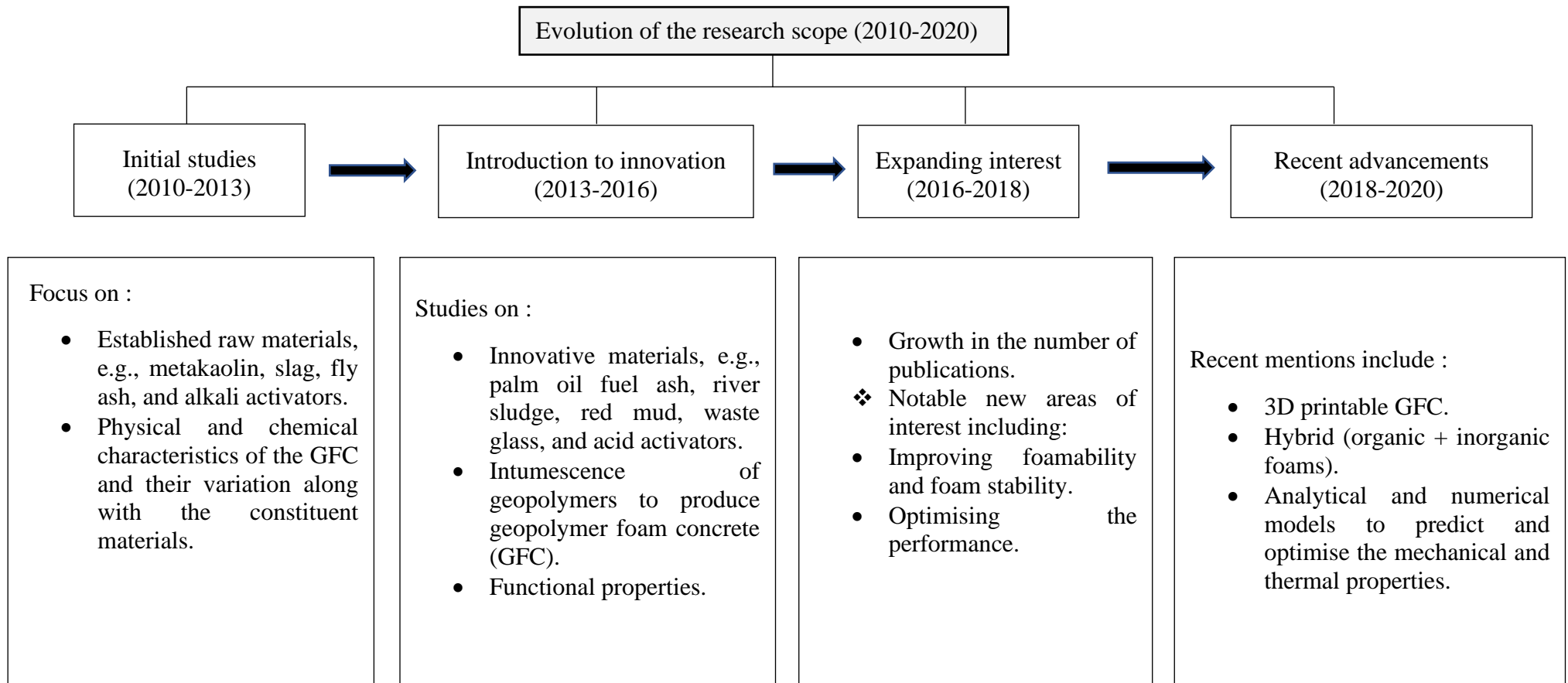


Figure 1- Evolution of the research scope, approximate timeline and notable mentions; adaptation from source

II.2.2 CHEMICAL STRUCTURE

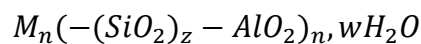
Geopolymers are macromolecules with an average molecular weight and particle size distribution similar to regular polymers [10]. As a matter of fact, Kriven et al. measured a molecular weight between 60,000 and 850,000 MW and particle dimensions between 5 and 15 nm for geopolymers [11].

J. Davidovits suggested poly(sialate) as chemical designation of geopolymers. The sialate, which is an abbreviation for silicon-oxo-aluminate, embodies a framework of SiO₄ and AlO₄ tetrahedrons alternately linked by sharing all oxygen atoms.

Having Al³⁺ in IV-fold coordination connected to 4 oxygen atoms generates a negative charge in the geopolymer [12]. To balance this charge, positive ions (like K⁺, Li⁺, Na⁺, Ca²⁺, Ba²⁺, NH³⁺ and H₃O⁺) must be present in the 3-D network cavities [10].

The intramolecular structure is predominated by ionic and covalent bonds, supported by Van Der Waals forces to form a cage-like microstructure [12].

The empirical formula of poly(sialates) is as following:



$z = \text{Si/Al ratio, } z = \{1,2,3\}$;

$M = \text{a monovalent cation like } K^+ \text{ or } Na^+$;

$n = \text{degree of polycondensation.}$

The aluminosilicate network's molecular structures are presented in the book of Davidovits, J., Inorganic polymeric new materials [6].

II.2.3 PROPERTIES

Geopolymers present a wide range of properties and characteristics besides their eco-friendly synthesis benefit, notably high compressive strength, low shrinkage, chemical corrosion resistance (which provides resistance to acid attack and to salts, such as chlorides and sulfates), fire resistance, fast setting, low thermal conductivity [4] and sound absorption [9]. Besides, geopolymers are stable up to 1000-1200 °C [10] and have the advantage of excellent durability at low cost [12].

Geopolymers present a microporous framework with porosity parameters depending on the quantity of foaming agent, the concentration of alkali activator and reaction temperature

[13]. They are synthesized at room temperature and discharge approximately 80% less CO₂ into the atmosphere than Portland cement during synthesis [4].

Owing to their zeolite-like structure, geopolymers are stable in water and can effectively adsorb heavy metals, dyes and other radioactive pollutants [14]. Furthermore, they have a large specific surface area, which can provide 4 to 5 times more ion exchange capacity than traditional adsorbents, such as activated carbon [15].

II.2.4 GEOPOLYMER APPLICATIONS

Geopolymer materials have gained a lot of interest as a prospective material for building restoration since their discovery, owing to their great characteristics, as well as in other fields [14].

The University of Queensland's Global Change Institute (GCI), built by HASSELL in cooperation with Bligh Tanner and Wagners, in 2013, is the world's first building to incorporate GPC in its structure. Rocla has successfully constructed and installed GPC sewer pipes, railway sleepers, cemetery crypts, box culverts and wall panels throughout Australia [16]. GPC was employed as an environmentally friendly paving grade substitute for Ordinary Portland concrete (OPC) in rigid pavement road construction and military bases [14]. Within a 7-day curing time, ecological ceramic tiles made from glass waste and metakaolin with an optimized ratio of SiO₂/Al₂O₃ = 4.0 reached recommended qualities for civil building operations. Similarly, metakaolin-based tiles performed well in high-temperature, ambient and saturation conditions [16]. Recent studies have also shown geopolymers' effectiveness as a 3D printing material [17].

Geopolymers have been exploited to separate dangerous metals in recent years. Fly ash-based geopolymer successfully prevented several dangerous metals, and the leaching rate was well compared to the Chinese standard. To conclude, producing geopolymers can not only be a way of converting waste solids into useful materials, but also contributes to environmental remediation by treating wastewater [14].

II.3 PRODUCTION

Geopolymerization is proved to be exothermic [10] (table 2), with kinetics depending on the type of raw material and its particle's fineness, curing temperature, solubility rate of the

solid particles in the alkaline solution, availability of the charge balancing ions and their type [9].

Table 2 - Calculated energy for different condensation reactions

Reactions	Energy [Kcal. mol ⁻¹]
$Si(OH)_4 + [Al(OH)_4]^- \rightarrow [SiOAl(OH)_6]^- + H_2O$	-27.0
$[Si_2O(OH)_6] + [SiOAl(OH)_6]^- \rightarrow [SiO_3AlO_4(OH)_8]^- + 2H_2O$	-11.3
$2SiO(OH)_4 \rightarrow [SiO(OH)_6] + H_2O$	-4.9
$2[Si_2O(OH)_6] \rightarrow [Si_4O_4(OH)_8] + H_2O$	-2.8
$2[Al(OH)_4]^- \rightarrow [Al_2OH(OH)_6]^- + OH^-$	41.1
$2[Al(OH)_4]^- \rightarrow [Al_2O(OH)_6]^{2-} + H_2O$	53.0

II.3.1 GEOPOLYMERIZATION PROCESS

Geopolymers are formed by condensing an aluminosilicate source in an alkaline meta-silicate solution at ambient temperature [4]. Although many studies have been conducted in the last decades on the geopolymerization mechanism, it is still not fully understood [8]. Geopolymerization is a geosynthetic process that relies on the capacity of aluminum ions to be incorporated (as an Al six-fold or four-fold coordination) into a silicate backbone [16]. In the 1950s, Glukhovsky presented a generalized mechanism for the alkali activation of materials mainly composed of silica and reactive alumina (Fig.2).

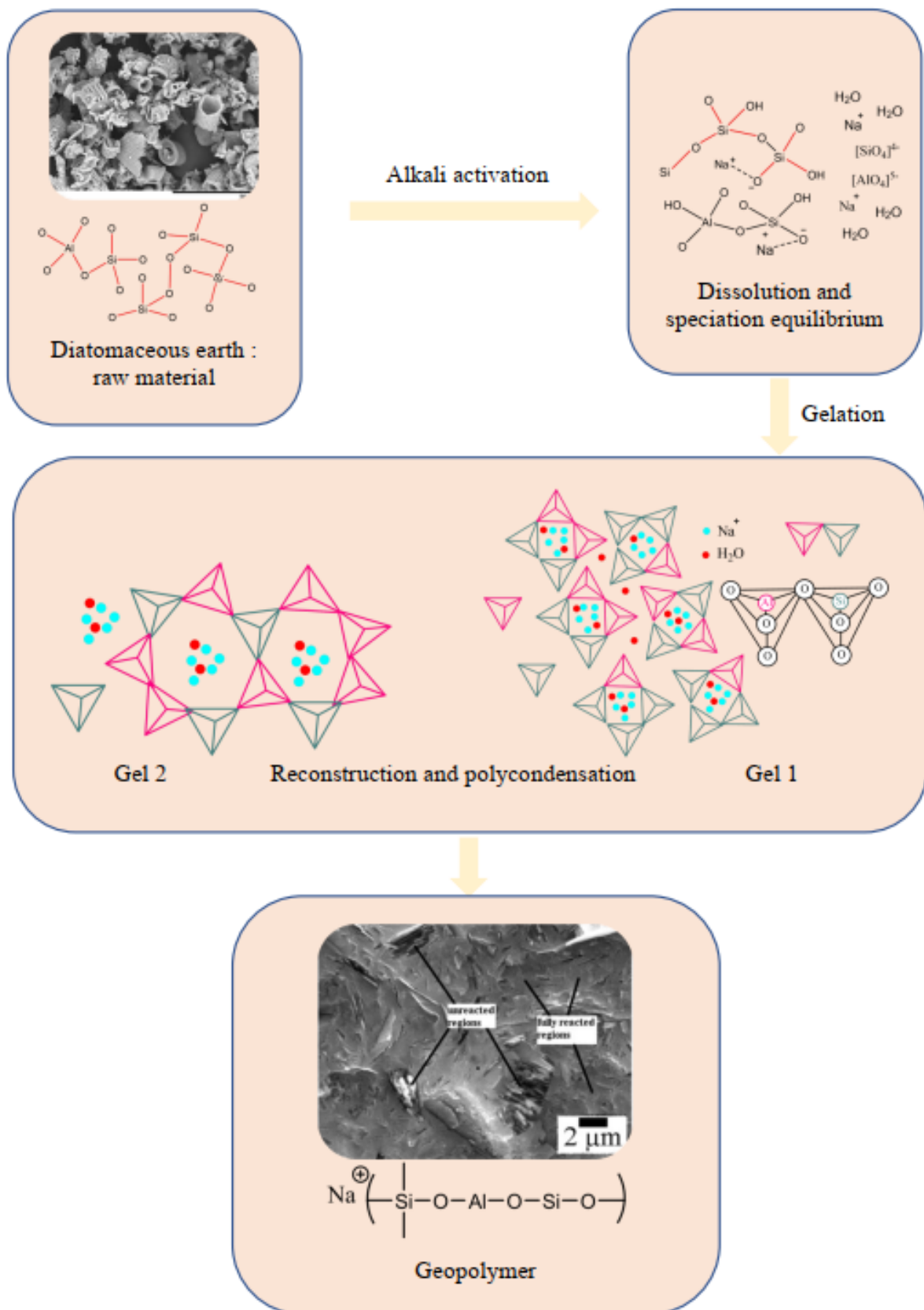


Figure 2 - Synthesis stages of geopolymers; adaptation from source

The process is divided into three phases by the Gluhovsky model [18]:

- Destruction–coagulation.
- Coagulation–condensation.
- Condensation–crystallization

The geopolymerisation process starts by the dissolution of the solid amorphous aluminosilicate source by alkaline hydrolysis, generating $\text{Si}(\text{OH})_4$ and $\text{Al}(\text{OH})_4^-$ monomers [18]. This occurs when the alkaline activator OH^- ions break the Si-O-Si bonds and transfer their electronic density to the silicon atoms weakening this way the other Si-O-Si bonds and making them more susceptible to rupture (Fig.3). This reaction produces silanol ($-\text{Si}-\text{OH}$) and silate ($-\text{Si}-\text{O}^-$) species, with the alkaline cations like Na^+ and K^+ balancing their negative charge and acting as catalysts. The presence of $\text{Si}-\text{O}^-$, Na^+ compounds limits the reverse reaction to Si-O-Si [19]. The Si-O-Al bonds are likewise affected by the OH^- groups releasing $\text{Al}(\text{OH})_4^-$ ions.

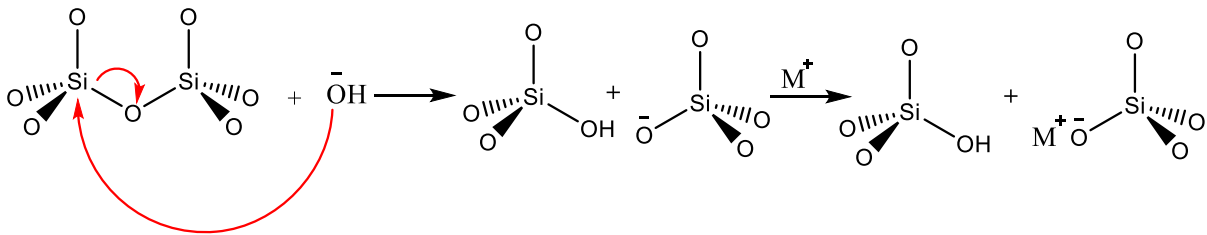


Figure 3 - Si-O-Si bond breakage mechanism by the reaction of OH^- ions; adaptation from source

In the condensation process, the reactive silicate and aluminate monomers bind via oxygen bridges to form dimers and so on to have a more cross-linked system [20]. During this process, water must be removed from the media to avoid hydrolysis (Fig.4). This stage is catalyzed by OH^- ions. The geopolymerization of the silicic acid and aluminates forms clusters that continue to grow in all directions yielding colloids [19]. The alkaline metal in this stage is a structural component [21].

These processes witness successive precipitation of 2 gels (Fig.5): Gel 1 and Gel 2.

Gel 1: an aluminum-rich gel.

Gel 2: a gel with a composition different from Gel 1, it is richer in silicates.

The dissolution of the aluminosilicate source leads at a certain stage to an Al-rich metastable sodium aluminosilicate hydrate (N-A-S-H) gel as an intermediate product. The

dissolution rate of the reactive aluminum exceeds that of silicon because Al-O bonds are weaker than Si-O bonds. Consequently, the richer the source material is in aluminum the quicker is the precipitation of the Gel 1, which results in a geopolymer richer in aluminum. With the progress of the reaction, more and more Si-O groups are dissolved, increasing the silicon content in the reaction media and its proportion in the N-A-S-H gel (Gel 2) [19].

The last process is the polycondensation and crystallization of the initial gels to form a geopolymer [20].

The reaction's kinetics in the first two processes play a key role in the formulation of final products, hence their physical and mechanical properties [16].

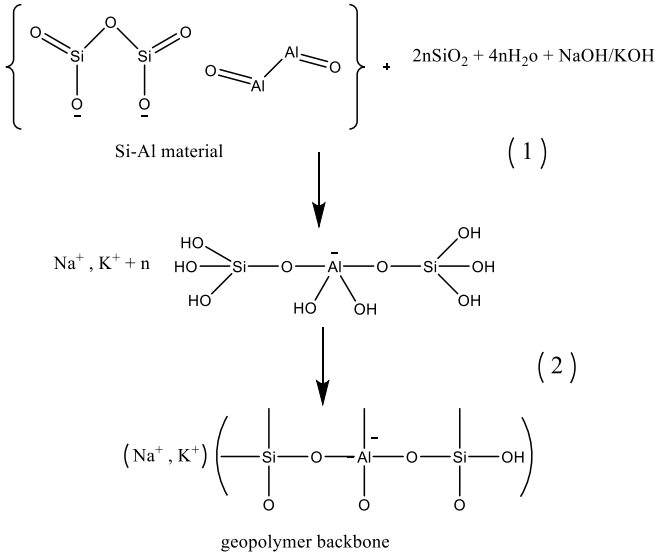


Figure 4 - Chemical equation of geopolymers synthesis; adaptation from source

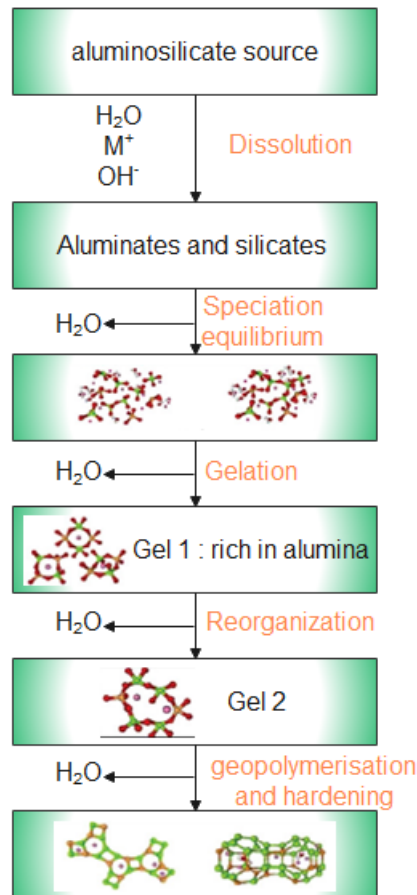


Figure 5 - Conceptual model of geopolymerization; adaptation from source

It is necessary to control the parameters that influence the synthesis process and the final product structure (Fig.6) so that geopolymers can achieve their application objectives and attain their optimal rheological and chemical properties.

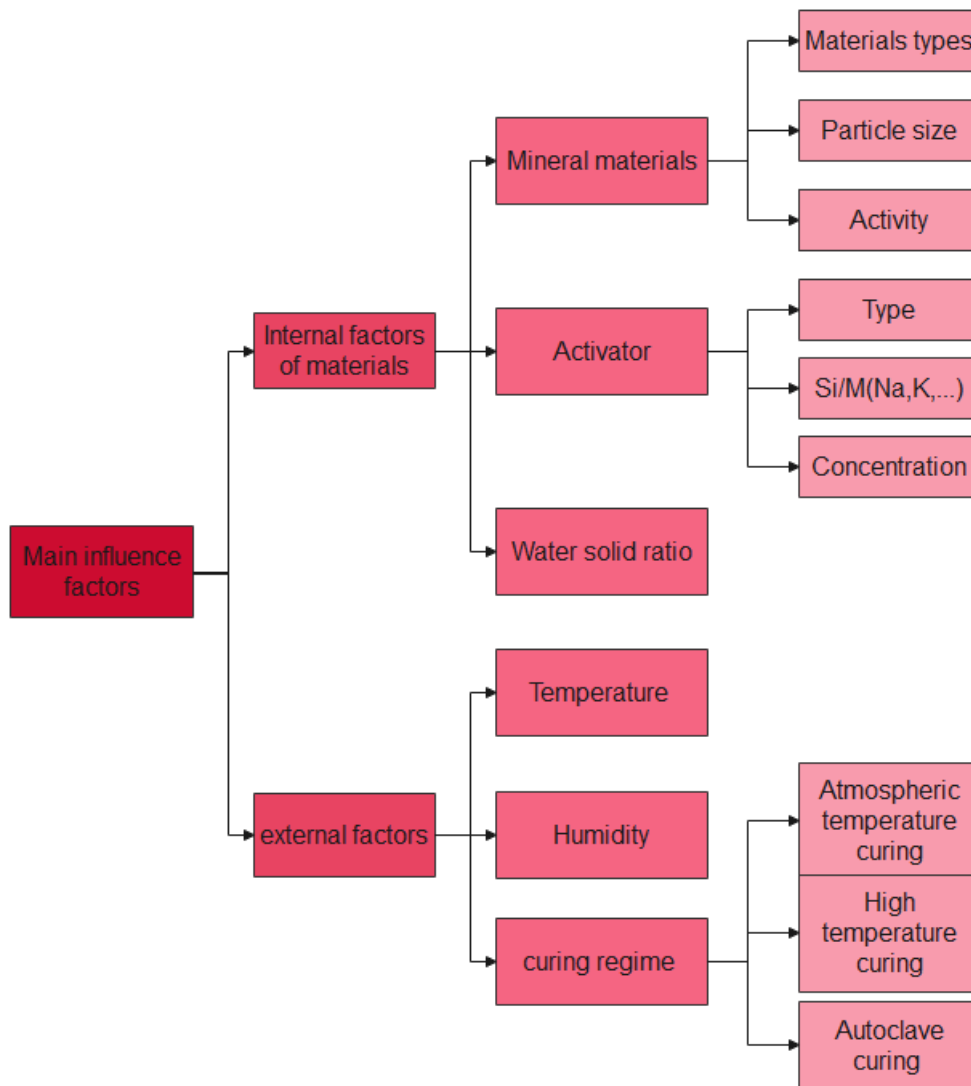


Figure 6 - Main factors influencing preparation of geopolymers; adaptation from source

II.3.2 RAW MATERIAL

Geopolymers can take natural materials and waste products as the primary raw materials synthesized by alkali or acid activation reaction [14]. However, the opportunity to exploit industrial waste as raw materials is valuable, especially in light of the emerging circular economy paradigm [22].

Calcined clay (metakaolin 750), fly ash, rice husk ash, slag, waste glass, diatomaceous earth, copper mine tailings, zeolite, red mud, pure $\text{Al}_2\text{O}_3\text{-}2\text{SiO}_2$ powder with Na_2SiO_3 , magnesium-containing minerals and palm oil fuel ash (POFA) from Malaysia are among the aluminosilicate raw materials used [16]. Waste sources can be categorized as shown in Fig.7.

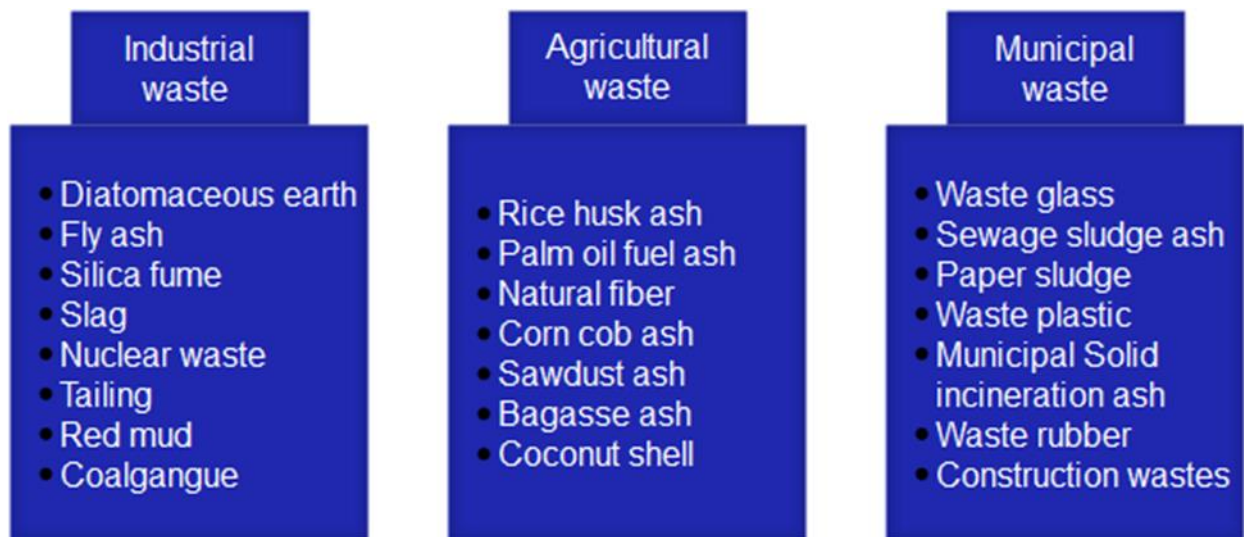


Figure 7 - Categories of waste sources that can be used as a precursor of geopolymers; adaptation from source

Table 3 summarizes some synthesis experiences that involve natural and waste diatomaceous earth as raw material.

Table 3 - Synthesis experiences of geopolymers using diatomaceous earth

Raw material	Composition (wt%)	Activating solution	Ratios	Curing T°	Curing time	Properties	ref
Residual diatomites from the wine and beer industry	Composition of wine industry residual diatomites SiO ₂ : 71.89/ Al ₂ O ₃ : 6.95/ Fe ₂ O ₃ : 1.77/ CaO: 1.2/ MgO: 0.26/ SO ₃ : 1.89/ K ₂ O: 2.58/ Na ₂ O: 1.33/ TiO ₂ : 0.45/ LOI: 11.05	NaOH + Na ₂ SiO ₃		20 °C	7-28 d		[5]
Diatomaceous earth + (mix of fly ash and metakaolin)		NaOH + Na ₂ SiO ₃	-L/S: 0.42 -Mix of fly ash and metakaolin: 70%+30% -SiO ₂ /Al ₂ O ₃ : 4.4 -Na ₂ O/SiO ₂ : 0.2	60 °C	28d 180d 360d	CS: 38 MPa	[23]
Diatomite	SiO ₂ :97.3/ Al ₂ O ₃ :1.596/ Fe ₂ O ₃ :0.355/ CaO: 0.154/ MgO:0.183/ K ₂ O: 0.299/ Na ₂ O: 0.073/ TiO ₂ : 0.034/ P ₂ O ₅ : 0.006	K ₂ SiO ₃	Geopolymer composition: K ₂ O•Al ₂ O ₃ •4SiO ₂ •11H ₂ O	- RT	UT	FS: 9.2 MPa CS: 71 MPa Weibull modulus: 5.4 Amorphous geopolymer	[4]

Calcium aluminat cement (CAC)+ diatomite		Na ₂ SO ₄ solid + NaOH 8M	CAC: 20% Diatomite: 80%	RT RH: 99%	Molded 24h and tested after two days of unmulding		[24]
Diatomaceous earth and rice husk ash	Diatomaceous earth's composition: SiO ₂ :77.46/ Al ₂ O ₃ :10.97/ Fe ₂ O ₃ :9.08/ CaO: 0.35/ MgO:0.31/ K ₂ O: 1.07/ TiO ₂ : 0.41/ LOI: 11.35	NaOH	SiO ₂ /Al ₂ O ₃ :13.0-33.5	75 °C	5 d	Bulk density: 0.88 g/cm ³ CS: 15 kg/cm ²	[25]

LOI: loss on ignition at 1000°C

RT: room temperature

T°: temperature

RH: relative humidity

II.3.3 ACTIVATING SOLUTIONS AND TYPICAL CONDITIONS

The names "geopolymer" and "alkali-activated materials" are constantly confused or used as synonyms. The difference between the terms geopolymers and alkali-activated materials is shown in Fig.8 [26].

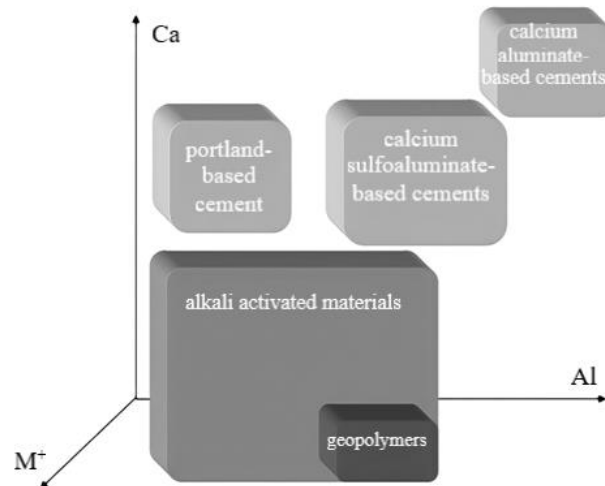


Figure 8 - Difference between cements, alkali activated materials and geopolymers according to their composition; adaptation from source.

II.3.3.1 Activating solutions

As activating solutions, most research has adopted alkali hydroxides, silicates or a combination of both [9], and the alkaline metals are typically potassium, sodium and, in few cases, calcium [27]. More distinctively, NaOH and KOH are the most frequently used alkaline activators. The concentration of NaOH in the geopolymeric system's aqueous phase influences the dissolving process and the bonding of solid particles in the final structure [28].

It has been reported that a 10 M concentration of NaOH leads to the highest dissolution rate of aluminosilicate material, inducing a higher degree of geopolymerization compared to lower concentrations of NaOH [14]. Nevertheless, effective activation was verified also employing borax ($\text{Na}_2\text{B}_4\text{O}_7 \cdot 10\text{H}_2\text{O}$), phosphoric acid (H_3PO_4), alkali carbonate and alkali aluminates [9]. Acid-base activated geopolymers had higher thermal resistance (up to 1450°C) and superior mechanical properties than alkali-base geopolymers [14].

Although they're cheap and accessible, sodium carbonate and sulfate are inefficient compared to hydroxides and silicates, yet according to the literature they're useful to correct the pH value when mixed with hydroxides [29]. Using silicate activators will provide a higher

concentration of Si in the medium. With alumina availability in the medium (Gel 1), the silicate activator's silica reacts with alumina, accelerating the geopolymerization process [30].

Studies have shown that using a mixture of silicate and sodium hydroxide activators may improve the strength of the geopolymer by 50 MPa compared to using only hydroxide [31]. Other studies showed that using Na_2SiO_3 as an activator can lead to values of strength of 90-100 MPa after 1 day of cure at 80°C whereas using only NaOH presents a geopolymer's resistance of 15-20 MPa [32].

In addition, compared to sodium silicate activators, hydroxide activators have the disadvantage of generating geopolymers with higher permeability and the possibility of efflorescence due to the excess of alkali metals and the weak Na bonds in the geopolymer [33]. The use of $\text{Na}_2\text{SiO}_3 \cdot 5\text{H}_2\text{O}$ solid activator reduces the water-binder ratio and gives a stronger product than using the common liquid activator because of the chemical combination of part of the water in the mixing phase with the undissolved particles of sodium metasilicate pentahydrate. The geopolymer activated by a composite activator is cleaner than that activated by Na_2SiO_3 or Na_2CO_3 . Previous research has revealed that sodium-based alkali activators have a higher activation efficiency for fine fly ash (FFA) than potassium-based activators. However, using potassium compounds in geopolymer systems resulted in higher alkalinity than using NaOH. As a solid activator, potassium carbonate (solid) is used. Since it also provides additional active aluminum, NaAlO_2 is a promising activator. Corollary, it's important to select activators based on the qualities of the raw materials. Activators can be made from solid waste or organic incinerator ash as well [14].

The molarity of hydroxides and the silica modulus (M_s) of the hydroxide and silicate are two of the most critical parameters in reaction kinetics. Eqs. (1) and (2) define these parameters [30].

$$M = \frac{n\text{NaOH}}{V} \quad \text{Eq (1)}$$

With:

M = molarity (in M);

nNaOH= number of moles of sodium (in moles);

V = solution's volume (in L).

$$Ms = \frac{nSiO_2}{nNa_2O} \quad \text{Eq (2)}$$

With:

M_s = silica modulus;

$nSiO_2$ = number of moles of silicon oxide (in moles);

nNa_2O = number of moles of sodium oxide (in moles).

II.3.3.2 Curing conditions

Curing temperature is critical for geopolymerization. The increase in temperature accelerates the dissolution of raw material, therefore, higher temperatures are advantageous for geopolymerization, as table A1 in the appendix cites some examples of curing temperatures used [14]. A slight temperature rise can significantly affect the synthesis rate [9].

The common curing methods of geopolymers are [17] :

- High-temperature curing
- Autoclave curing
- Microwave curing

Due to its fast and penetrating heating abilities, microwave radiation was demonstrated to be an effective technology for synthesizing geopolymers, the power used is usually between 200W and 900W. In fact, microwave energy stimulates additional geopolymerization by evaporating excess free water, allowing geopolymers to reach higher strength in less time [14].

Though autoclave curing is less economical to reduce cracks and improve strength, it is widely used yet with temperatures ranging between 20°C and 300°C. Experience shows that autoclave curing is a more appropriate method for the system that has a low concentration of Na_2O and low SiO_2/Na_2O ratio [17].

Curing in oven extends curing time, resulting in partial evaporation of water and the creation of microcavities, leading to an easily cracked sample and drastically altering the reactions. Alkaline activation is inhibited at temperatures above 100°C due to a lack of moisture in the samples. This rapid water loss causes carbonation, which delays the activation of precursors, resulting in a high aluminum content in the gels that develops. In this case, the final product is porous and mechanically weak. As a result, thermal curing at moderate temperatures, around 60–70°C, and for short periods, up to 7 days, is the best option [21].

II.3.3.3 Foaming

Foamed geopolymers, also known as foam/foamed, aerated, cellular, or porous geopolymers or GFC, are formed by incorporating sizable voids/pores into the geopolymer slurry or mortar.

Ground granulated blast furnace slag (GGBS), class F fly ash (5% CaO by weight) and metakaolin are the most often used aluminosilicates in the production of GFC. GFC was also synthesized using bottom ash, class C fly ash (>5% CaO by weight), river sludge, mining wastes, waste glass, soil, palm oil fuel ash and coconut ash. Studies have shown viscosity's influence on the foaming degree, lower viscosity generating a better-foamed structure than a viscous base mix [9].

Innovative foaming agents and techniques were adopted in multiple research:

- Chemical foaming: voids are created in chemical foaming by a gas-releasing reaction in the fresh base mix, which, when set, results in a cellular structure. Multiple foaming agents were used, such as metals (Al, Zn, Si), H₂O₂ and carbonate.
- Mechanical foaming: generating in situ detergent inside the fresh geopolymer mix by a saponification process. Several mechanical foaming agents have studied: vegetable and animal sources of fatty acids, such as vegetable oil, sunflower oil, castor oil or beef tallow.
- Intumescence of solid geopolymer: when alkali-activated solids with a high Si/Al ratio (>20) are heated, they expand to produce a porous structure. Microwave irradiation was proven effective as a technique to emphasize the geopolymer's intumescence behavior.
- Other ways of making porous geopolymers include replicating, using a sacrificial filler, and using additive manufacturing [9].

II.4 ADSORBENT CHARACTER OF GEOPOLYMERS FOR WATER TREATMENT

The development of low-cost, environmentally friendly adsorbents, such as waste-based geopolymers, is a captivating strategy to depollute industrial wastewater and contribute to cleaner manufacturing. This is because their synthesis may be conducted with a relatively low energy and low amount of activating solution, without greenhouse gas emissions and with solid waste raw material. Furthermore, due to the strong binding of the pollutants to the geopolymer

matrix, their remanufacture after exhaustion in other applications (e.g., as filler or aggregate in the production of new building materials) is possible and simple, which provides significant advantages over the benchmark adsorbent activated carbon, that has extremely high production costs and whose recovery after use is challenging [14]. The capacity of geopolymers to exchange cations with the solution has made them recognized as a promising alternative to activated carbons [34]. Geopolymers can take different shapes to perform as adsorbent material: powder, bulk type form and monolithic bodies (e.g., membranes). Monolithic bodies have captivated the scientific community's interest, as this is a safer and easier strategy than using nano- or micro-sized geopolymer powders. Some research used a metakaolin-based geopolymer cylindrical membrane to extract Ni^{2+} from a synthetic effluent without needing a post-separation step. Other research used cylindrical discs to recover lead from wastewaters [22]. Multiple research projects have reported the efficiency of geopolymers as adsorbents regarding their surface area and adsorption capacity. Table 4, [35], summarizes some of the results obtained using geopolymers as adsorbents.

Table 4 - Previous studies on the adsorption of dyes and heavy metals with geopolymers

Adsorbate		Adsorbent	Surface area (BET) m ² /g	Average pore diameter (nm)	Adsorption capacity Q _{max} (mg/g)	pH	Regeneration
Dyes	Methylene blue	Metakaolin-Based Geopolymer			43.48		
		Phosphoric acid based geopolymers	33.39	8.61	2.84		5 cycles
		FA-based geopolymer spheres			30.1		8 cycles
		Biomass FA-geopolymer monoliths			15.4		5 cycles
	Methyl-violet	Mesoporous geopolymer	62	14.3	276.9		
	Methyl Orange	Metakaolin based Geopolymer			0.3393		
Cu (II)	Organic modified metakaolin-based geopolymer	26.45	9.12	108.2			
	Porous geopolymeric spheres	53.95	5.38	52.63	5		

Heavy metals		Geopolymer/ alginate hybrid spheres	16.2	11.5	60.8±2.3	5	
		Porous metakaolin-based inorganic polymer sphere	26.45	9.12	147.1	5	
		Metakaolin based geopolymers	35		44.73		
		Fly ash and iron ore tailing-based geopolymers			113.4		
	Zn (II)	Metakaolin based geopolymer	39.24		74.53		
		Red Earth			8.74		
		Natural Volcanic Tuff-based geopolymer powder			14.7	7	
		Metakaolin-based geopolymer powder	65.7		147.06	4	
		Metakaolin-based geopolymers powder	35		74.36	6-7	
	Ni (II)	Metakaolin based geopolymer	39.24		42.61		
		Geopolymer derived from blast furnace slag powder	30.84	11.86	85.29	10	

		Metakaolin-based geopolymer powder			42.61	7.25	
		Geopolymer microspheres	10.46		414.38	5	
	Pb (II)	Porous inorganic polymer	100.99	7	629.21		
		Red Earth			10.31		
		Fly ash-based geopolymer powder			183.605	4	
		Fly ash-based geopolymer powder	20.48	19.62	118.6	3	
		Geopolymer microspheres	100.99	7	629.21	4	
	Cd (II)	Metakaolin-based geopolymer	65.7		75.74		
		Metakaolin geopolymer powder	8.16		70.3	5	
		Metakaolin-based geopolymer	5.7		67.57	4	
		Zeolite-based geopolymer	130.45		26.245	5	
	Cr (VI)	CTAB modified geopolymers (Single system)	26.45	9.12	61.3		

During the production of geopolymers, the product has to be washed with water until a neutral pH to prevent the hydroxides' precipitation and to maintain the adsorption efficiency. Adsorption is the deposition and retention of a solid or gaseous solute on a solid's surface and interface. There are two adsorption processes: physical adsorption (physisorption) and chemical adsorption (chemisorption). Physisorption consists of the binding of the adsorbate and the adsorbent by energetically low bonds like Van Der Waals forces or equivalent forces, e.g., hydrogen bonds, electrostatic polarization interactions and dipole-dipole interaction π - π , among others. Consequently, it's a reversible reaction. Chemisorption consists of forming strong chemical bonds between the adsorbate and the adsorbent, including exchanging electrons, which is a usually irreversible reaction. It's characterized by forming a monomolecular layer (monolayer) on the surface of the solid adsorbent. For example, in geopolymers, the negative charge of the Al tetrahedron ($-\text{Si}-\text{O}-\text{Al}-\text{O}-\text{Si}-\text{O}$) can be responsible for the chemisorption process in the presence of cation adsorbates.

Adsorption mechanisms can be elucidated based on isotherms and kinetic studies.

II.4.1 ADSORPTION KINETICS

Adsorption kinetics exhibit the rate of adsorption and depicts the adsorption mechanism. Three adsorption kinetic models are used to characterize the adsorption mechanism: pseudo-first order, pseudo-second order and intra-particle diffusion models. Pseudo-first order model speculates that physisorption is the control step of the adsorption mechanism. The pseudo-second-order kinetic model is generally applied to describe the chemisorption type adsorption phenomena. Table 5, [35], summarizes some geopolymer adsorption experiences with their correspondent kinetic model.

Table 5 : Kinetics and isotherm studies of the adsorption of dyes and heavy metals with geopolymers based on different raw materials.

Adsorbate		Adsorbent	Kinetic model	Isotherm model
Dyes	Methylene blue	Porous gangue microsphere/ geopolymer composites	Pseudo-second order	Langmuir
	Basic yellow 2	Fly ash-based geopolymer	The pseudo-second order and the intra- particle diffusion	Langmuir and Temkin
	Methylene blue	Metakaolin-Based Geopolymer	Pseudo-second order	Langmuir
	Methyl orange	Activated Geopolymer	Pseudo-second order	Langmuir
	Methylene blue	Geopolymer	Pseudo-second order	Langmuir
	Methyl violet 10B	Mesoporous geopolymer	Pseudo-second order	
	Methylene blue	Perlite-Based Geopolymer	Pseudo-second order	
	Methylene blue	Phosphoric acid-based geopolymers	Pseudo-second order	Langmuir
Heavy metals	Cu (II)	Fly ash-based geopolymers	Pseudo-second order	Langmuir
	Ni (II)	Geopolymer microspheres	Pseudo-second order	Langmuir
	Cs (I)	Mesoporous geopolymers	Pseudo-first and second-order model	Langmuir
	Pb (II)	Gold mine tailings-based geopolymer	Pseudo-second order	Langmuir
	Mn(II), Co(II)	Metakaolin based geopolymer	Pseudo-second order	Langmuir

	Zn (II), Ni(II)	Metakaolin based geopolymer	Pseudo-second order	Langmuir
	Cu (II), Cd (II), Zn (II), and Pb (II)	Hollow gangue microsphere/geopolymer	Pseudo-second order	Langmuir
	Pb (II), Cu (II), Cr (II), and Cd (II)	Metakaolin-based geopolymer	Pseudo-second order	Langmuir

II.4.2 ADSORPTION ISOTHERMS AND MECHANISMS

Adsorption isotherms describe the relationship between the equilibrium concentration of the adsorbate and the maximum adsorbed quantity at the solid's surface. They describe the phase as well formed at the adsorbent surface, which can be a monolayer or a multilayer. Four adsorption isotherm models are typically used to characterize the layer formed on the surface, the integration of the adsorbate and to evaluate the adsorption capacity, namely Langmuir, Freundlich, Temkin and Dubinin-Radushkevich models.

The Langmuir model describes the formation of a monolayer on a homogenous adsorbent surface that contains a finite number of identical sites. The Freundlich isotherm characterizes a multilayer formation on an adsorbent's heterogeneous surface. The Temkin model describes the interaction between the adsorbent and the adsorbate and the heat of the adsorption process of all molecules in the layer. In table 5, it's shown some of the adsorption process isotherm models associated with experiences carried out in some research works.

METHODOLOGY

III. METHODOLOGY

III.1 REACTANTS

The reactants described below were used in this work for geopolymer preparation and adsorption testing.

- Geopolymer's preparation

Diatomaceous earth (DE), supplied by Campelo (Company). Sodium hydroxide (NaOH), provided by Labbox (Barcelona, Spain). Sodium silicate (Na_2SiO_3), supplied by fisher scientific (Loughborough, United Kingdom) (Na_2O , ~10.6% SiO_2 , ~26.5%). Alumina (Al_2O_3), supplied by thermos scientific (Darmstadt, Germany). Distilled water, provided with pH=6.5.

- Adsorption testing

Phenol ($\text{C}_6\text{H}_6\text{O}$) and gallic acid ($\text{C}_6\text{H}_2(\text{OH})_3\text{CO}_2\text{H}$) with more than 98% purity, purchased from Merck (Darmstadt, Germany).

All solutions used in the experiments were prepared in distilled water.

III.2 GEOPOLYMER'S PREPARATION

The amounts of SiO_2 and Al_2O_3 of the commercial diatomaceous earth were around 70% and 18.5%, respectively, according to Campelo company. The precursors for geopolymer synthesis should have a high amount of SiO_2 . The high amount of SiO_2 (70%) suggests that diatomaceous earth can be considered a valuable material for preparing geopolymers whether an appropriate method is used.

For the preparation of the geopolymer, formulations were planned according to different mass ratios of reactants with different curing conditions to explore their effect on the geopolymer's properties and performance as an adsorbent. The formulas were prepared according to Table 6. The curing process of each sample was different. Samples 1-13 were first placed in a wet chamber during 7 days at 25 °C with a humidity of 95%. Then samples were left at room temperature during different periods of time:

1. Samples 1-2: 2 months.
2. Samples 3-7: 5 weeks.
3. Sample 8: 32 days.
4. Sample 9: 10 days.
5. Sample 10: 9 days.
6. Sample 11: 3 days.
7. Sample 12: 2 days.
8. Sample 13: 1 day.

Table 6 - Formulas used to produce geopolimer samples.

Sample	DE (g)	Al ₂ O ₃ (g)	Na ₂ SiO ₃ (g)	NaOH (g)	H ₂ O ₂ (μL)	H ₂ O (mL)	Si/Al (molar)
1	130	37	100	9	0	450	2
2	130	37	40	12	0	450	1.55
3	103	52	135	59.8	250	200	1.67
4	117	58	105	70	250	225	1.4
5	93	47	126	84	250	210	1.7
6	117	58	131	43.75	250	260	1.6
7	93	47	158	52.5	250	141	1.9
8	123	62	115	50.9	250	137	1.4
9	90	45	149	66.3	250	165	1.9
10	103	52	106	88.8	250	222	1.5
11	103	52	149	45.1	250	112	1.8
12	103	52	135	59.8	250	150	1.7
13	103	52	135	59.8	250	150	1.7
14	103	52	135	59.8	250	150	1.7
15	23.7	4.8	31.6	0.15	0.6	32	3.1
16	23.7	4.8	0	16	0	51	1.6
17	23.7	4.8	22.5	13.83	0	45	2.7
18	23.7	4.8	15	13.83	0	50	2.3
19	23.7	4.8	33	13.83	0	40	3.2
20	23.7	4.8	33	13.83	0.6	55	3.2
21	23.7	4.8	31.6	0	0	15.8	3.1
22	23.7	4.8	31.6	0	0	15.8	3.1
23	23.7	4.8	31.6	0	0	32	3.1

24	23.7	4.8	31.6	0	0	32	3.1
25	23.7	4.8	31.6	0	0	47.3	3.1
26	23.7	4.8	31.6	0	0	47.3	3.1

Afterward, samples 1-13 were put in an oven at 40 °C for 5 days.

Sample 14 was cured only at ambient temperature; samples 15 and 21-26 were cured for 2 days in the wet chamber, then, in the oven at 40 °C; and samples 16-20 were cured only in the oven at 40 °C for 6 days.

Each geopolymer was prepared using two mixtures separately. The amounts of diatomaceous earth and alumina indicated in Table 6 were mixed and stirred for 10 minutes. Likewise, the amounts of sodium silicate and sodium hydroxide solutions were mixed and stirred for 10 min at 200 rpm resulting in the activating solution. Then, the activating solution and the predefined quantity of hydrogen peroxide were added into the solid mixture. Afterwards, the mixture was stirred while adding the minimum amount of water (if needed) until it became a homogeneous paste, as shown in Fig.9. The stirring process can take from 40 to 120 min, depending on the amount of each compound added.

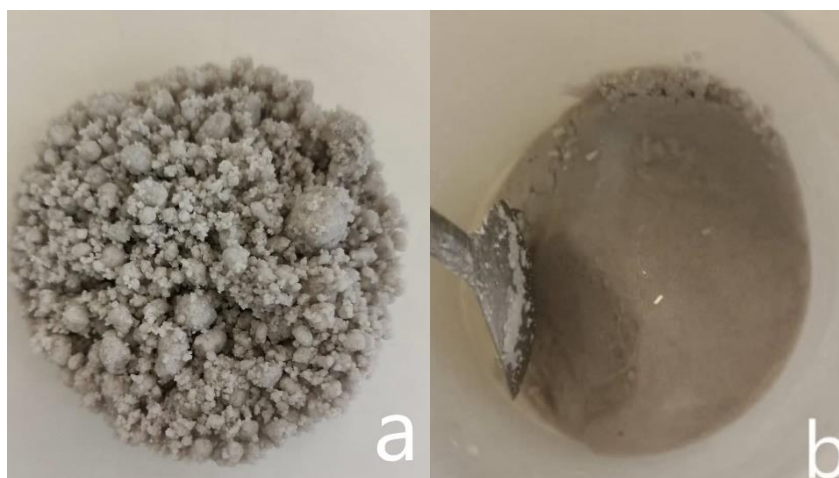


Figure 9 - Example of a geopolymer sample (a) during and (b) after stirring.

Afterward, the samples were introduced in a mold of rectangular shape (40 × 40 × 160 [mm]) and cured. After curing, the geopolymer sample that had solid shape was crushed to be tested as an adsorbent in powder form and then sieved to obtain particle sizes ranging between 106 and 250 μm.

The powder was then washed with a continuous flow of distilled water at ambient temperature until the washing water reached a neutral pH. The washed sample was put in oven at 40 °C for 24 h and then stored for further analysis and adsorption tests.

III.3 CHARACTERIZATION OF GEOPOLYMERS

III.3.1 CHARACTERISATION OF THE GEOPOLYMER AS POWDER MATERIAL :

After crushing, sieving, washing and drying, the geopolymer sample was analyzed by physisorption and Fourier-transform infrared spectroscopy (FT-IR).

Brunauer-Emmett-Teller (BET) theory aims to explain the physical adsorption of gas molecules on a solid surface and serves as the basis for an important analysis technique for the measurement of the specific surface area of materials. BET theory applies to systems of multilayer adsorption, and usually utilizes probing gases that do not chemically react with material surfaces as adsorbates to quantify specific surface area. Nitrogen is the most commonly employed gaseous adsorbate used for surface probing by BET methods. For this reason, standard BET analysis is most often conducted at the boiling temperature of N₂ [36].

BET surface area results were obtained using QuantaChrome NOVA touch LX4 equipment. Fourier-transform infrared spectra were obtained using a Perkin-Elmer spectrophotometer over a scan range of 450-2000 cm⁻¹ at room temperature.

III.3.2 APPLICATION OF GEOPOLYMER AS ADSORBENT IN POWDER FORM

The geopolymer samples were intended to be tested as adsorbents for gallic acid and phenol removal. A study of adsorption capacity and isotherms was carried out.

III.3.2.1 QUANTIFICATION METHOD OF GALLIC ACID AND PHENOL SOLUTIONS

The amount of gallic acid and phenol adsorbed was quantified by using a UV/Vis spectrophotometer (Jasco V530 spectrophotometer). First, the maximum absorbance wavelength was determined for both components, and then calibration curves were performed at 260 and 270 nm [37] for gallic acid and phenol, respectively.

For aqueous phenol solution, the calibration curve is shown in Fig.10.

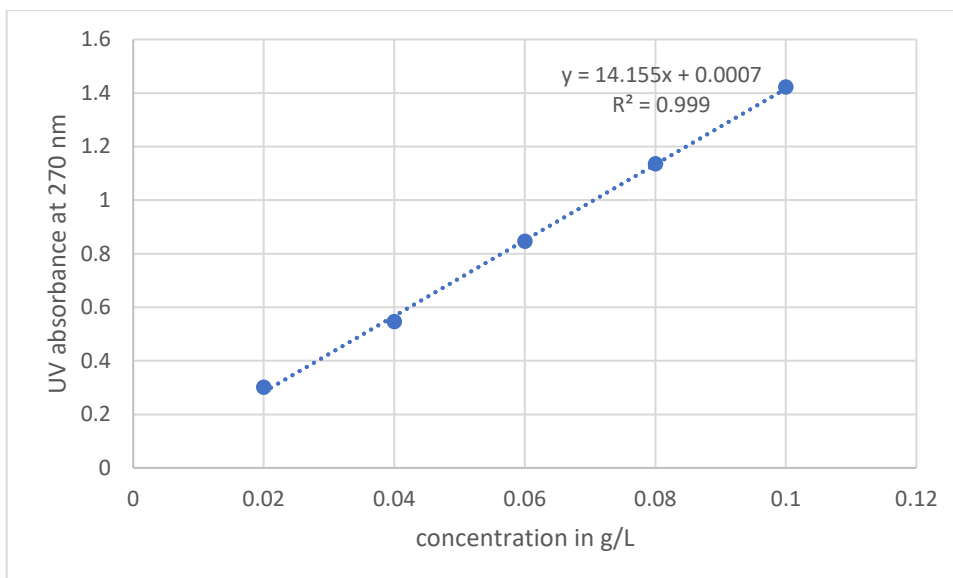


Figure 10 - Phenol calibration curve by UV/Vis spectrophotometry using a wavelength of 270 nm.

For aqueous gallic acid solution, the calibration curve is shown in Fig.11.

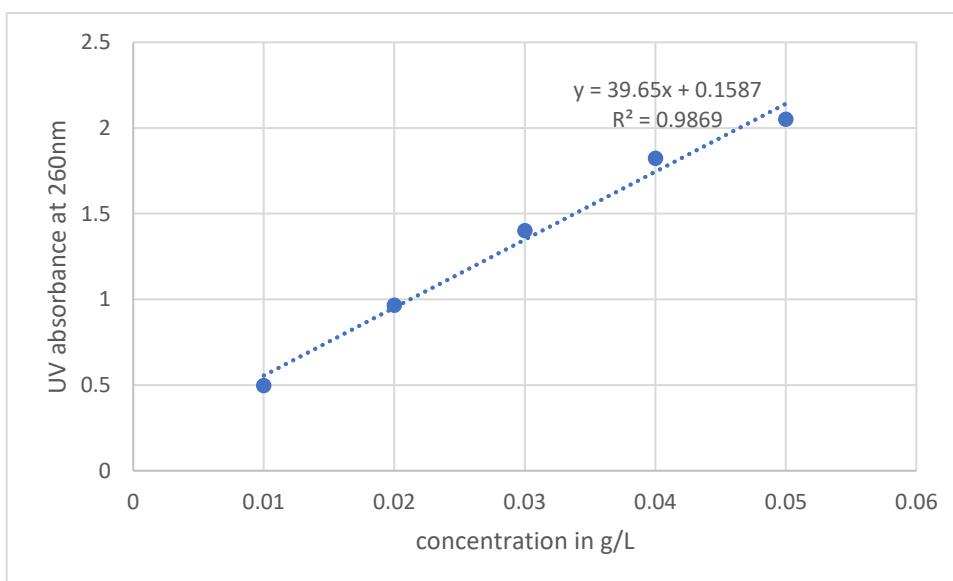


Figure 11 - Gallic acid calibration curve by UV/Vis spectrophotometry using a wavelength of 260 nm.

III.3.2.2 PRELIMINARY ESSAYS

A preliminary adsorption test was carried out to check whether the geopolymer is ready to be considered as an adsorbent and to get an idea about the adsorption capacity. In two

different Erlenmeyers, 50 mg of the washed and dried geopolymer powder sample was introduced with 10 mL of gallic acid 0.1 g/L in one Erlenmeyer and 10 mL of phenol 0.1 g/L in the other Erlenmeyer. Then, both erlenmeyers were placed in an orbital shaker at 250 rpm for 72 h at 25 °C (Fig.12).



Figure 12 - Agitation of the geopolymer samples in adsorbate solutions in the orbital shaker

Afterward, the solutions were filtered, and the recovered liquid was measured by UV/Vis spectrophotometry in order to quantify the phenol and gallic acid, whereas the geopolymer was measured by FT-IR.

III.3.2.3 ADSORPTION ISOTHERMS STUDY

The adsorption isotherms of gallic acid and phenol on geopolymers were studied through seven suspensions, which were prepared in erlenmeyers with different loads of geopolymer (50-110 mg) and 10 mL of the adsorbate solutions 0.1 g/L. The erlenmeyers were placed in an orbital shaker at 250 rpm for 72 h at 25 °C. Afterward, the solutions were filtered and gallic acid and phenol concentration determined by UV/Vis spectrophotometry.

The adsorption capacity of the geopolymer was determined as q_e (quantity of adsorbate (mg) per adsorbent (g) at equilibrium stage, reached at 72 h). It was calculated using equation (3) [38].

$$q_e = \frac{(C_0 - C_e) * V}{m_{geopolymer}} \quad (3)$$

where C_0 and C_e refer to the adsorbate concentration in the aqueous solution (mg/L) at the beginning and the equilibrium stages, respectively; V is the volume of the aqueous solution and $m_{geopolymer}$ refers the mass of the adsorbent used in each experiment.

The removal, R (%), of the pollutant in the experiments was measured as the percentage of the adsorbate on the geopolymer; according to equation (4) [38].

$$R = \frac{(C_0 - C_e) * 100}{C_0} \quad (4)$$

RESULTS AND DISCUSSION

IV. RESULTS AND DISCUSSION

IV.1 APPEARANCE OF THE GEOPOLYMERS

According to the formulas and the curing mode planned to produce the geopolymers, the results compiled in Table A2 (in appendix) were obtained. Samples 1 and 2 contain excessive water that floated on the top after the mixing process. Excessive water leads to the dilution of the activating solution and with water floating on top there was evaporation leading eventually to loss of a portion of the activator. The samples' aspects can indicate a very low geopolymerization degree. To remedy this issue all the other samples were produced with a minimum volume of water just sufficient to turn the mix into a paste.

The aspects of samples 3- 14 are very similar. This is due to the low Si/Al molar ratio, knowing that silicon is the element responsible for geopolymer's strength. Given that calcination may change the crystallinity of DE and have the potential of converting six-coordinated aluminum into four-coordinate species [39], sample 12 was the sample that was produced using calcined diatomaceous earth (calcination was made at 800 °C for 2 h). The result obtained was no different from the one produced with non-calcined diatomaceous earth using the same formula under the same conditions.

Sample 13 was divided into 2 parts, one part cured at ambient temperature, the other part cured first in wet chamber for 7 days, then at ambient temperature. Both shapes are significantly different, the part that cured only at ambient temperature had a dry solid shape, whereas the other one was not solid. Hence, it can be concluded that the curing mode chosen (7 days in wet chamber, then curing at ambient temperature) is not suitable.

Sample 15 was produced with the minimum amount of water, it has a Si/Al ratio of around 3, very low concentration of sodium hydroxide and was left only 2 days in wet chamber then cured in oven at 40 °C. It presented the best shape as solid compared to all other samples.

Samples 21-26 (Fig.13) were produced in order to study the influence of sample's thickness, while curing, on its final form and to optimize the volume of water added. Samples 21 and 22 differ only by their thickness; it is also the case for samples 23 and 24, also for 25 and 26 (Fig. 14).



Figure 13 - Samples 21-26 before curing process.

By comparing samples 22, 24 and 26, it can be concluded that the amount of water is optimal for sample 24. Comparing samples 25 and 26, it can be concluded that the samples thickness is a key factor that controls the sample's final state. Sample 26 is one phased dry solid whereas sample 25 presents a bright transparent solid layer on top (looks like glass) and dark on the inside. Hence, the dark color observed in the previous samples and their separation into two phases can be due to their thickness.



Figure 14 - Samples 21-26 after 2 days in wet chamber and 3 days in oven.

According to the previous results, sample 15 was chosen to be treated and tested as an adsorbent since it has the best sample among all regarding its solid shape. The drying period was identified by controlling the weight loss of the geopolymer. After 5 days in the oven at 40 °C, the geopolymer's mass became constant at $m = 43.34 \text{ g}$.

IV.2 pH EVOLUTION IN GEOPOLYMERS WASHING

A piece of sample 15 (the piece's mass = 15.8 g) was collected, crushed and sieved, giving the following particle size (\emptyset) distribution:

$$\emptyset > 250 \mu\text{m} \Rightarrow m = 3.337 \text{ g}$$

$$250 \mu\text{m} > \emptyset > 106 \mu\text{m} \Rightarrow m = 3.087 \text{ g}$$

$$106 \mu\text{m} > \emptyset \Rightarrow m = 9.341 \text{ g}$$

Then, the sample with particle sizes between 106 and 250 μm was washed using 11 L of distilled water (pH 6.5) while controlling the pH, as shown in Fig.15, until the washing water had a pH 7.3. Then, the sample was dried in oven for 24 h at 40 °C (Fig.16).

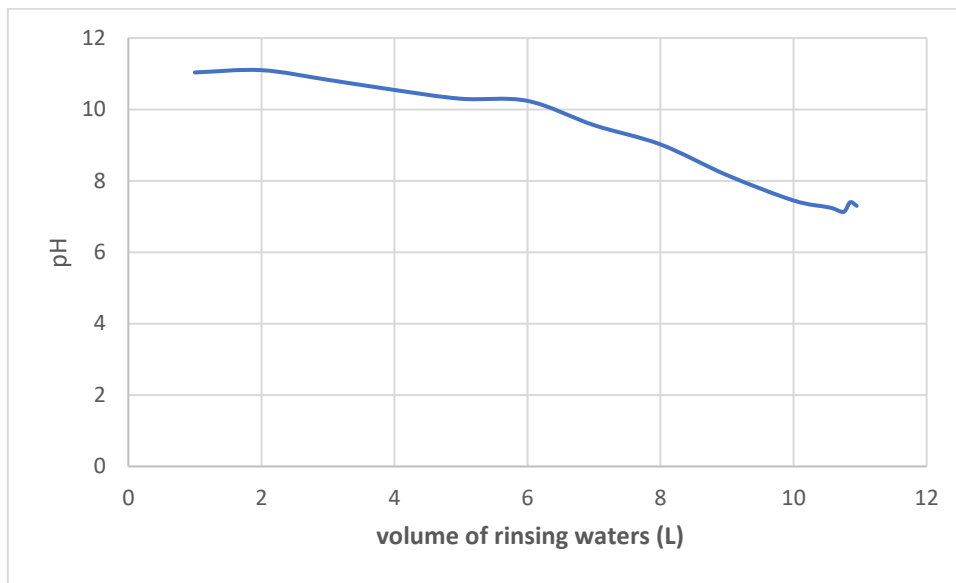


Figure 15 – pH evolution of the rinsing water during washing geopolymers.



Figure 16 - Geopolymer sample after drying.

After washing and drying, the geopolymer lost mass and 15.2% was recovered in the process. These mass losses can be explained by:

- a. Dissolution of geopolymer particles when the media was basic: this geopolymer sample was proved to be not stable at high pH. Indeed, an experience was made by placing a non-washed sample in distilled water for 24 h, and it dissolved, as shown in Fig.17. The pH of water was around 11.



Figure 17 - Non-washed geopolymer sample 15 placed in distilled water for a day.

- b. Presence of very small particles in the powder that were dragged along by water through the filter paper while washing with a continuous flow of distilled water
- c. Particles were lost during the sample manipulation and washing and drying in the oven processes.

IV.3 CHARACTERIZATION OF THE SELECTED GEOPOLYMER

The geopolymer sample 15 was measured by physisorption with nitrogen to determine the BET surface area, giving a result of $32 \text{ m}^2/\text{g}$, which is considered low knowing that one gram of activated carbons have specific surface areas of $500\text{-}1300 \text{ m}^2/\text{g}^{-1}$ [40]. The FT-IR spectrum of the geopolymer sample, after washed and dried, is presented in Fig.18.

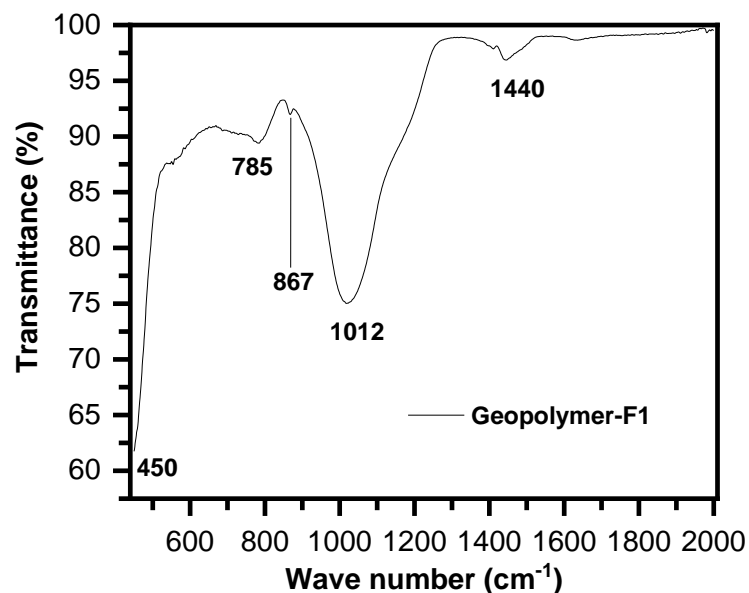


Figure 18 - FT-IR spectrum of the geopolymer sample 15 after washing and drying.

The band at 1012 cm^{-1} is attributed to Si-O-Si stretching, the band at 785 cm^{-1} is associated with Si-O bending, and the band at 450 cm^{-1} is due to Si-O rocking. The intense peak at 1012 cm^{-1} indicates the great presence of Si-O bonds which favors the theory of geopolymer production. (Stretching and rocking are types of molecular vibrations in IR spectroscopy) [41].

IV.4 APPLICATION RESULTS OF THE GEOPOLYMER SAMPLE AS ADSORBENT IN POWDER FORM

At the end of the washing process, washing water was measured by UV/Vis spectrophotometry at wavelengths of 260 and 270 nm, and the absorbance values were around 0, which proves that, in the adsorption test, the UV/Vis absorbance values of adsorbate solutions at 260 and 270 nm are characterizing only gallic acid and phenol.

IV.4.1 PRELIMINARY TEST RESULTS

After 72 h spent in the phenol solution, the geopolymer sample was still solid and the solution was clear in both erlenmeyers. The pH of the phenol solution after the adsorption test was 7.9, whereas the pH of the gallic acid solution after the adsorption test was 6.07 Table 7 presents the adsorption results.

Table 7 - Equilibrium concentration of the adsorbate in solution (C_e), equilibrium uptake capacity (q_e) and Removal (R) obtained in the adsorption of gallic acid and phenol on the geopolymer.

Pollutant	C_e (mg/L)	q_e (mg/g)	R (%)
Gallic acid	59	8.4	41
Phenol	98	0.384	1.92

These results show that the geopolymer sample is efficiently adsorbent for gallic acid, since uptake capacity in the equilibria reached 8.4 mg/g, whereas for phenol adsorption it is considered not efficient ($q_e = 0.384$ mg/g).

The FT-IR spectrum (spectrum 1) of the geopolymer sample after being used in gallic acid adsorption is presented in Fig.19.

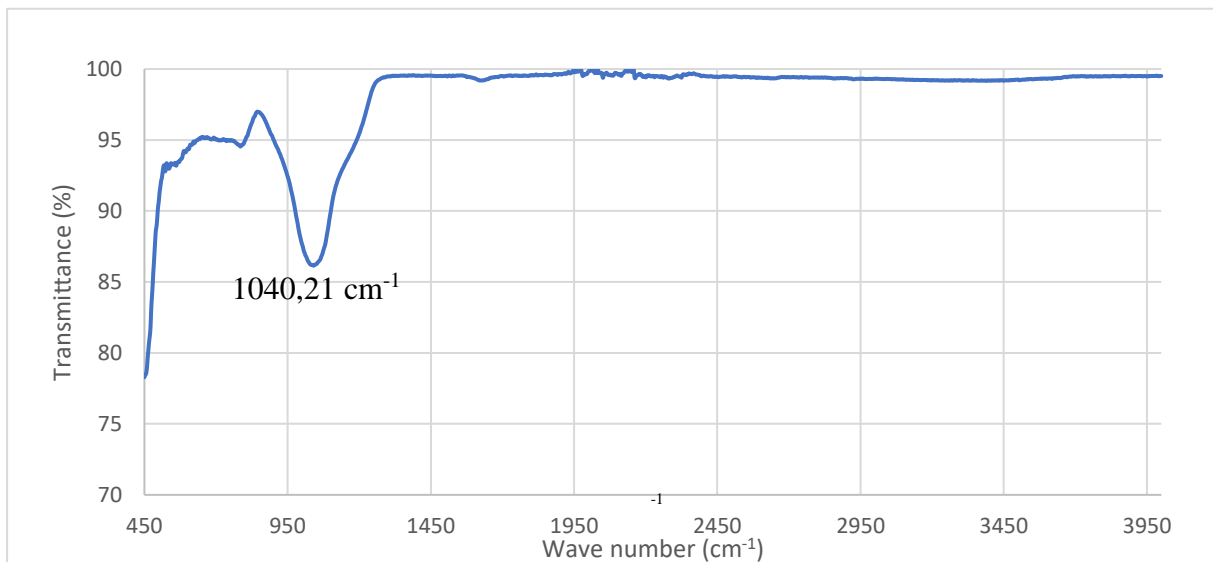


Figure 19 - FT-IR spectrum of geopolymer sample after the gallic acid adsorption test.

The FT-IR spectrum (spectrum 2) of the geopolymer sample after being used for adsorption of phenol is presented in Fig.20.

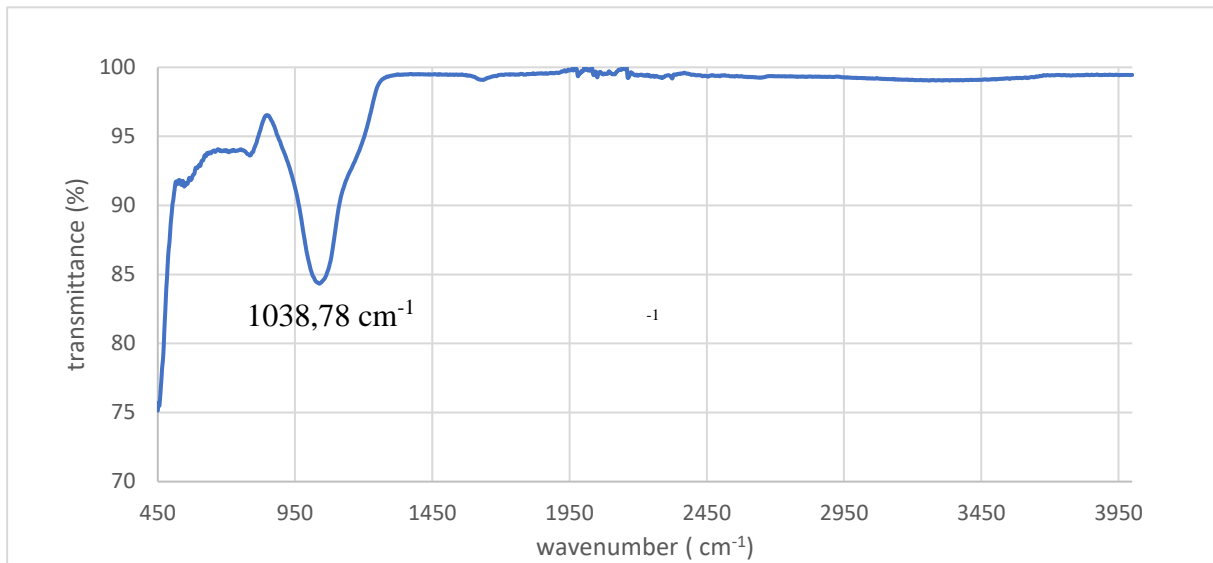


Figure 20 - FT-IR spectrum of the geopolymer sample after the phenol adsorption test.

Both FT-IR spectra are similar; the band at 1040.21 cm^{-1} in spectrum 1 and at 1038.78 cm^{-1} in spectrum 2 are assigned to Si-O stretching. These spectrums show no difference with the geopolymer sample spectrum done before the adsorption test.

IV.4.2 ADSORPTION ISOTHERMS

The results of the isotherm test for gallic acid adsorption are shown in Table 8 and Fig.21.

Table 8 - Isotherm data for gallic acid adsorption

Run	C_0 (mg/L)	geopolymer mass (mg)	Absorbance*	C_e (g/L)	q_e (mg/g)
1	100	50	0.308	0.054	-
2	100	60	0.3569	0.065	5.78
3	100	70	0.332	0.06	5.76
4	100	80	0.321	0.057	5.35
5	100	90	0.294	0.051	5.44

6	100	100	0.268	0.045	5.48
7	100	110	0.343	0.062	3.44

*absorbance values determined at 260 nm for the samples diluted 10 times.

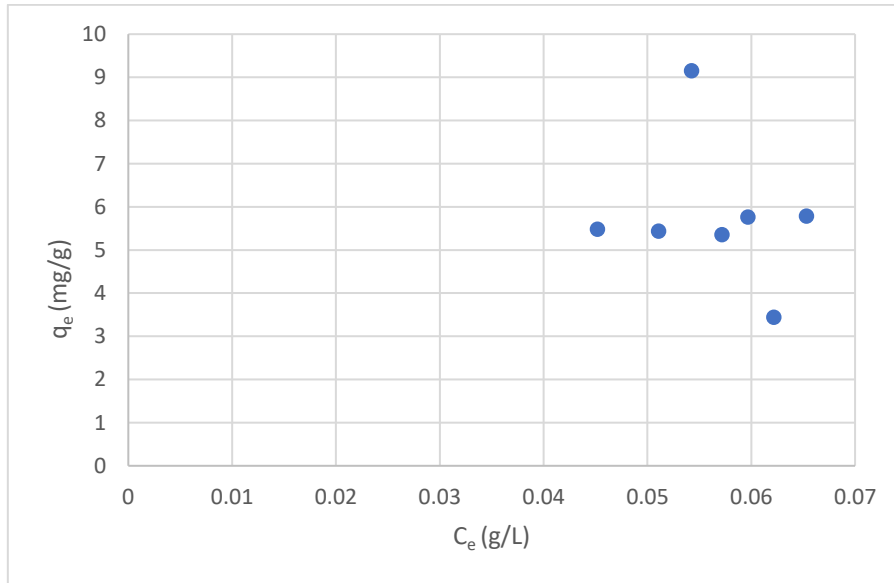


Figure 21 - Isotherm of gallic acid adsorption.

The results of the isotherm test for phenol adsorption are shown in Table 9 and Fig.22.

Table 9 - Isotherm data for phenol adsorption

Run	C_0 (mg/L)	geopolymer mass (mg)	Absorbance*	C_e (g/L)	q_e (mg/g)
1	100	50	1.509	0.1	19.7
2	100	60	1.58	0.11	16.4
3	100	70	1.597	0.11	14
4	100	80	1.592	0.11	12.3
5	100	90	1.542	0.1	10.9
6	100	100	1.597	0.11	9.8
7	100	110	1.598	0.11	8.9

*absorbance values determined at 270 nm

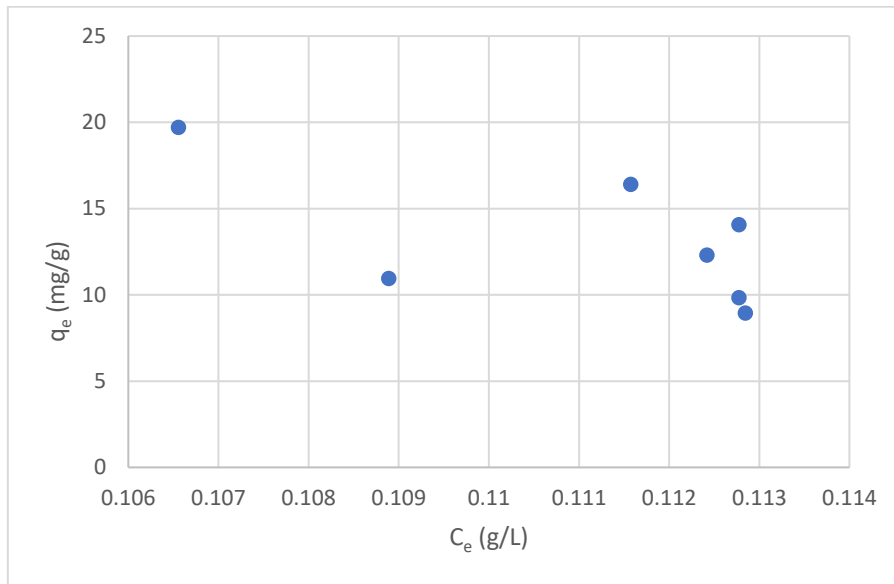


Figure 22 - Isotherm of phenol adsorption

In Fig.23, it's represented the different isotherm curve shape of each type of adsorption process [42].

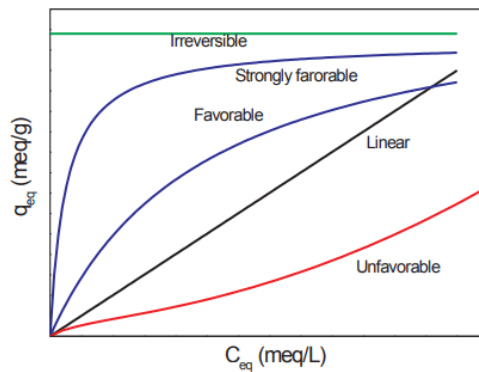


Figure 23 - Isotherm curve shape

We can observe that increasing the amount of adsorbent with the same adsorbate concentration gives insignificant curve shapes, which can indicate that the geopolymer material is still not stable enough in an aqueous media and that it may be releasing some components that are in the origin of the inexplicable UV absorbance values. Considering these isotherms, It can be concluded that the geopolymer sample is not adsorbent, and that it's not stable in an aqueous media.

CONCLUSION AND OUTLOOKS

V. CONCLUSIONS AND OUTLOOKS:

During the course of this project, it has been carefully examined the literature around wastewater treatment using diatomaceous earth-based geopolymers. An approach of the potential adsorption model of geopolymers was established. Considering that waste diatomaceous earth may contain unknown impurities, it was suggested to proceed first with using commercial diatomaceous earth and studied the feasibility of geopolymer making.

For this purpose, many experiences were made to finally create an optimal protocol to synthesize a geopolymer material using commercial diatomaceous earth. Through this optimization process, we could already establish a preferable thickness of the geopolymer within the curing mold as well as an optimal molar ratio of $\text{Si/Al} = 3$ with the removal of NaOH as activator. The result of this geopolymerization was then put to test for adsorption of gallic acid and phenolic compounds. The results of isotherm studies indicated that the geopolymer is still not stable enough in an aqueous media to allow a significant adsorption.

This opens new avenues for improvement based on studies of clay-based geopolymers. Indeed, this cheap geopolymer material's performance can be further enhanced by the addition of metakaolin while keeping the overall cost inferior to that of using clay-based geopolymers on their own. What's more, observing its curing process and its behavior when exposed to high temperature implies that this material can be resistant to heat transfer. Furthermore, this material is porous, which allows it to present a good thermal and sound isolator material.

REFERENCES

VI. REFERENCES

1. Davidovits, J., *Geopolymer Chemistry and Application* 2019.
2. Oliveira, M. and E. Duarte, *Integrated approach to winery waste: waste generation and data consolidation*. *Frontiers of Environmental Science & Engineering*, 2016. **10**(1): p. 168-176.
3. *Wine Crush: How Diatomaceous Earth Plays a Role in Wine Making · Dicalite Management Group*. Available from: <https://www.dicalite.com/2017/11/wine-crush-how-diatomaceous-earth-plays-a-role-in-wine-making/>.
4. Bagci, C., G.P. Kutyla, and W.M. Kriven, *Fully reacted high strength geopolymer made with diatomite as a fumed silica alternative*. *Ceramics International*, 2017. **43**(17): p. 14784-14790.
5. Font, A., et al., *Use of residual diatomaceous earth as a silica source in geopolymer production*. *Materials Letters*, 2018. **223**: p. 10-13.
6. Davidovits, J., *Inorganic polymeric new materials*. *Thermal analysis* 1991. **37**: p. 1633-1656.
7. imarc. 2021; Available from: <https://www.imarcgroup.com/geopolymer-market/toc>.
8. Provis, J.L. and J.S.J. Van Deventer, *Introduction to geopolymers*, in *Geopolymers*. 2009. p. 1-11.
9. Dhasindrakrishna, K., et al., *Progress, current thinking and challenges in geopolymer foam concrete technology*. *Cement and Concrete Composites*, 2021. **116**: p. 103886.
10. Davidovits, J., *Geopolymers and geopolymeric materials*. *Journal of Thermal Analysis*, 1989. **35**: p. 429-441.
11. Waltraud, M.K., L.B. Jonathon, and M. Gordon, *Microstructure and microchemistry of fully reacted geopolymers and geopolymer matrix composites* The American Ceramic Society, 2003.
12. Ren, B., et al., *Eco-friendly geopolymer prepared from solid wastes: A critical review*. *Chemosphere*, 2021. **267**: p. 128900.
13. Zawrah, M.F., et al., *Fabrication and characterization of non-foamed and foamed geopolymers from industrial waste clays*. *Ceramics International*, 2021. **47**(20): p. 29320-29327.
14. Cong, P. and Y. Cheng, *Advances in geopolymer materials: A comprehensive review*. *Journal of Traffic and Transportation Engineering (English Edition)*, 2021. **8**(3): p. 283-314.
15. Wei, E., et al., *Preparation and conversion mechanism of different geopolymer-based zeolite microspheres and their adsorption properties for Pb²⁺*. *Separation and Purification Technology*, 2022. **282**.
16. Srividya, T., et al., *A state-of-the-art on development of geopolymer concrete and its field applications*. *Case Studies in Construction Materials*, 2022. **16**.
17. Zhao, J., et al., *Eco-friendly geopolymer materials: A review of performance improvement, potential application and sustainability assessment*. *Journal of Cleaner Production*, 2021. **307**.

18. Duxson, P., et al., *Geopolymer technology: the current state of the art*. Journal of Materials Science, 2006. **42**(9): p. 2917-2933.
19. Palomo, A., et al., *A review on alkaline activation: new analytical perspectives*. Materiales de Construcción, 2014. **64**(315).
20. Wu, Y., et al., *Geopolymer, green alkali activated cementitious material: Synthesis, applications and challenges*. Construction and Building Materials, 2019. **224**: p. 930-949.
21. De Oliveira, L.B., et al., *Durability of geopolymers with industrial waste*. Case Studies in Construction Materials, 2022. **16**: p. e00839.
22. Novais, R.M., R.C. Pullar, and J.A. Labrincha, *Geopolymer foams: An overview of recent advancements*. Progress in Materials Science, 2020. **109**.
23. Mejia, J.M., R.M.d. gutierrez., and C. Montes., *Rice husk ash and spent diatomaceous earth as a source of silica to fabricate a geopolymeric binary binder* Cleaner Production 2016. **118**: p. 133-139.
24. Arbi, K., A. Palomo, and A. Fernández-Jiménez, *Alkali-activated blends of calcium aluminate cement and slag/diatomite*. Ceramics International, 2013. **39**(8): p. 9237-9245.
25. Pimraksa, K., et al., *Lightweight geopolymer made of highly porous siliceous materials with various Na₂O/Al₂O₃ and SiO₂/Al₂O₃ ratios*. Materials Science and Engineering: A, 2011. **528**(21): p. 6616-6623.
26. Provis, J.L. and S.A. Bernal, *Geopolymers and Related Alkali-Activated Materials*. Annual Review of Materials Research, 2014. **44**(1): p. 299-327.
27. Provis, J.L., *Alkali-activated materials*. Cement and Concrete Research, 2018. **114**: p. 40-48.
28. Somna, K., et al., *NaOH-activated ground fly ash geopolymer cured at ambient temperature*. Fuel, 2011. **90**(6): p. 2118-2124.
29. Mendes, B.C., et al., *Application of eco-friendly alternative activators in alkali-activated materials: A review*. Journal of Building Engineering, 2021. **35**.
30. Marvila, M.T., A.R.G.d. Azevedo, and C.M.F. Vieira, *Reaction mechanisms of alkali-activated materials*. Revista IBRACON de Estruturas e Materiais, 2021. **14**(3).
31. Fernández-Jiménez, A. and A. Palomo, *Composition and microstructure of alkali activated fly ash binder: Effect of the activator*. Cement and Concrete Research, 2005. **35**(10): p. 1984-1992.
32. Altan, E. and S.T. Erdoğan, *Alkali activation of a slag at ambient and elevated temperatures*. Cement and Concrete Composites, 2012. **34**(2): p. 131-139.
33. Najafi Kani, E., A. Allahverdi, and J.L. Provis, *Efflorescence control in geopolymer binders based on natural pozzolan*. Cement and Concrete Composites, 2012. **34**(1): p. 25-33.
34. Rafatullah, M., et al., *Adsorption of methylene blue on low-cost adsorbents: a review*. J Hazard Mater, 2010. **177**(1-3): p. 70-80.
35. El Alouani, M., et al., *Application of geopolymers for treatment of water contaminated with organic and inorganic pollutants: State-of-the-art review*. Journal of Environmental Chemical Engineering, 2021. **9**(2).

36. MohammadSajadiZahraIssaabadi, M., *Chapter 6 - Plant-Mediated Green Synthesis of Nanostructures: Mechanisms, Characterization, and Applications*, in *Interface Science and Technology*. 2019. p. 199-322.
37. *NIST Standard Reference Database 69: NIST Chemistry WebBook*.
38. Gouamid, M., M.R. Ouahrani, and M.B. Bensaci, *Adsorption Equilibrium, Kinetics and Thermodynamics of Methylene Blue from Aqueous Solutions using Date Palm Leaves*. Energy Procedia, 2013. **36**: p. 898-907.
39. Tahmasebi Yamchelou, M., et al., *Geopolymer synthesis using low-grade clays*. Construction and Building Materials, 2021. **268**.
40. B.V., L. *Charbon Actif - Poudre ou grain* Available from: <https://www.lenntech.fr/francais/charbonactif-grain-poudre.htm>.
41. E. San Andre´s, A.d.P., F. L. Martı´nez, and I. Ma´rtıl, *Rapid thermal annealing effects on the structural properties and density of defects in SiO₂ and SiNx:H films deposited by electron cyclotron resonance*. 1999.
42. Piccin, J.S., Cadaval, T.R.S., de Pinto, L.A.A., Dotto, G.L. (2017). Adsorption Isotherms in Liquid Phase: Experimental, Modeling, and Interpretations. In: Bonilla-Petriciolet, A., Mendoza-Castillo, D., Reynel-Ávila, H. (eds) *Adsorption Processes for Water Treatment and Purification*. Springer, Cham. https://doi.org/10.1007/978-3-319-58136-1_2.
43. Abdollahnejad, Z., et al., *Mix design, properties and cost analysis of fly ash-based geopolymer foam*. Construction and Building Materials, 2015. **80**: p. 18-30.
44. Korat, L. and V. Ducman, *The influence of the stabilizing agent SDS on porosity development in alkali-activated fly-ash based foams*. Cement and Concrete Composites, 2017. **80**: p. 168-174.
45. Liu, Y., et al., *A facile method for preparation of floatable and permeable fly ash-based geopolymer block*. Materials Letters, 2016. **185**: p. 370-373.
46. Š. František, Š.R., T. Zdeněk, et al, *Preparation and properties of fly ash-based geopolymer foams*. Ceram.-Silik, 2014. **52**: p. 188-197.
47. Zhao, Y., et al., *Preparation of sintered foam materials by alkali-activated coal fly ash*. J Hazard Mater, 2010. **174**(1-3): p. 108-12.
48. Hajimohammadi, A. and J.S.J.v. Deventer., *Characterisation of one-part geopolymer binders made from fly ash*. 2017: p. 225-233.
49. Choo, H., et al., *Compressive strength of one-part alkali activated fly ash using red mud as alkali supplier*. Construction and Building Materials, 2016. **125**: p. 21-28.
50. Ban, C.C., P.W. Ken, and M. Ramli, *Mechanical and Durability Performance of Novel Self-activating Geopolymer Mortars*. Procedia Engineering, 2017. **171**: p. 564-571.
51. Matakah, F., et al., *Mechanochemical synthesis of one-part alkali aluminosilicate hydraulic cement*. Materials and Structures, 2016. **50**(1).
52. Nematollahi, B., J. Sanjayan, and F.U.A. Shaikh, *Comparative deflection hardening behavior of short fiber reinforced geopolymer composites*. Construction and Building Materials, 2014. **70**: p. 54-64.

53. van Riessen, A., et al., *Bayer-geopolymers: An exploration of synergy between the alumina and geopolymer industries*. Cement and Concrete Composites, 2013. **41**: p. 29-33.
54. Hajimohammadi, A., J.L. Provis, and J.S.J. van Deventer, *Effect of Alumina Release Rate on the Mechanism of Geopolymer Gel Formation*. Chemistry of Materials, 2010. **22**(18): p. 5199-5208.
55. Hajimohammadi, A., et al., *Regulating the chemical foaming reaction to control the porosity of geopolymer foams*. Materials & Design, 2017. **120**: p. 255-265.
56. Hlaváček, P., et al., *Inorganic foams made from alkali-activated fly ash: Mechanical, chemical and physical properties*. Journal of the European Ceramic Society, 2015. **35**(2): p. 703-709.
57. Böke, N., et al., *New synthesis method for the production of coal fly ash-based foamed geopolymers*. Construction and Building Materials, 2015. **75**: p. 189-199.
58. Ducman, V. and L. Korat, *Characterization of geopolymer fly-ash based foams obtained with the addition of Al powder or H₂O₂ as foaming agents*. Materials Characterization, 2016. **113**: p. 207-213.
59. Masi, G., et al., *A comparison between different foaming methods for the synthesis of light weight geopolymers*. Ceramics International, 2014. **40**(9): p. 13891-13902.
60. Feng, J., et al., *Development of porous fly ash-based geopolymer with low thermal conductivity*. Materials & Design (1980-2015), 2015. **65**: p. 529-533.
61. M.L. Gualtieri, A.C., M. Romagnoli, *Interactive powder mixture concept for the preparation of geopolymers with fine porosity*. European Ceramic Society, 2016. **10**: p. 2641-2646.
62. Muthu Kumar, E. and K. Ramamurthy, *Influence of production on the strength, density and water absorption of aerated geopolymer paste and mortar using Class F fly ash*. Construction and Building Materials, 2017. **156**: p. 1137-1149.
63. Sanjayan, J.G., et al., *Physical and mechanical properties of lightweight aerated geopolymer*. Construction and Building Materials, 2015. **79**: p. 236-244.
64. Nematollahi., B. and J.G. Sanjayan., *Ambient temperature cured one-part engineered geopolymer composite: a sustainable alternative to engineered cementitious composite* 2016.
65. Fernández-Jiménez, A., et al., *Sustainable alkali activated materials: Precursor and activator derived from industrial wastes*. Journal of Cleaner Production, 2017. **162**: p. 1200-1209.
66. Moraes, J.C.B., et al., *Increasing the sustainability of alkali-activated binders: The use of sugar cane straw ash (SCSA)*. Construction and Building Materials, 2016. **124**: p. 148-154.
67. Geraldo, R.H., L.F.R. Fernandes, and G. Camarini, *Water treatment sludge and rice husk ash to sustainable geopolymer production*. Journal of Cleaner Production, 2017. **149**: p. 146-155.
68. Wang, L. and X. Tan, *Preparation and properties of alkali activated foam cement reinforced with polypropylene fibers*. Journal of Wuhan University of Technology-Mater. Sci. Ed., 2011. **26**(5): p. 960-964.

69. Esmaily, H. and H. Nuranian, *Non-autoclaved high strength cellular concrete from alkali activated slag*. Construction and Building Materials, 2012. **26**(1): p. 200-206.
70. Zhang, Z., et al., *Mechanical, thermal insulation, thermal resistance and acoustic absorption properties of geopolymer foam concrete*. Cement and Concrete Composites, 2015. **62**: p. 97-105.
71. Kamseu, E., et al., *Cumulative pore volume, pore size distribution and phases percolation in porous inorganic polymer composites: Relation microstructure and effective thermal conductivity*. Energy and Buildings, 2015. **88**: p. 45-56.
72. Yang, K.-H., et al., *Properties and sustainability of alkali-activated slag foamed concrete*. Journal of Cleaner Production, 2014. **68**: p. 226-233.
73. Dembovska, L., et al., *The use of different by-products in the production of lightweight alkali activated building materials*. Construction and Building Materials, 2017. **135**: p. 315-322.
74. Vaou, V. and D. Panias, *Thermal insulating foamy geopolymers from perlite*. Minerals Engineering, 2010. **23**(14): p. 1146-1151.
75. Liu, M.Y.J., et al., *Evaluation of thermal conductivity, mechanical and transport properties of lightweight aggregate foamed geopolymer concrete*. Energy and Buildings, 2014. **72**: p. 238-245.
76. Zaidi, S.F.A., et al., *Synthesis & characterization of natural soil based inorganic polymer foam for thermal insulations*. Construction and Building Materials, 2017. **157**: p. 994-1000.
77. Roviello, G., et al., *Lightweight geopolymer-based hybrid materials*. Composites Part B: Engineering, 2017. **128**: p. 225-237.
78. Ye, J., W. Zhang, and D. Shi, *Properties of an aged geopolymer synthesized from calcined ore-dressing tailing of bauxite and slag*. Cement and Concrete Research, 2017. **100**: p. 23-31.
79. Humad, A.M., J.L. Provis, and A. Cwirzen, *Alkali activation of a high MgO GGBS – fresh and hardened properties*. Magazine of Concrete Research, 2018. **70**(24): p. 1256-1264.
80. Clausi, M., et al., *Reuse of waste sandstone sludge via alkali activation in matrices of fly ash and metakaolin*. Construction and Building Materials, 2018. **172**: p. 212-223.
81. Zaharaki, D., M. Galetakis, and K. Komnitsas, *Valorization of construction and demolition (C&D) and industrial wastes through alkali activation*. Construction and Building Materials, 2016. **121**: p. 686-693.
82. Novais, R.M., et al., *Waste glass from end-of-life fluorescent lamps as raw material in geopolymers*. Waste Manag, 2016. **52**: p. 245-55.
83. Gao, X., et al., *Characterization and application of municipal solid waste incineration (MSWI) bottom ash and waste granite powder in alkali activated slag*. Journal of Cleaner Production, 2017. **164**: p. 410-419.
84. Tekin, I., *Properties of NaOH activated geopolymer with marble, travertine and volcanic tuff wastes*. Construction and Building Materials, 2016. **127**: p. 607-617.

VII. APPENDIX

Table A1 - Synthesis experiences of geopolymers from waste sources

precursor: waste source	Chemical composition of waste source wt%	Activator	Additives	Ratios by wt %	Curing T°	Curing time	properties	Ref
Fly ash	SiO ₂ : 49,12 Al ₂ O ₃ : 27,3 Fe ₂ O ₃ : 8,19 CaO: 2,36 MgO: 1,42 SO ₃ : 1,3 K ₂ O: 3,34 Na ₂ O: 0,99 TiO ₂ : 2,32	Na ₂ SiO ₃ + NaOH	-NaBO ₃ : Chemical FA -H ₂ O ₂ : Chemical FA	-Na ₂ SiO ₃ / NaOH: 2.5, 3.5, 4.5. -Activator/ binder: 0.6, 0.8, 1.0. CFA: 1%, 2%, 3%	20°C	UT	CS: 4.6–6.89 MPa rho: 750–1350 kg/m ³	[43]
	SiO ₂ : 52.5 Al ₂ O ₃ : 23.3 Fe ₂ O ₃ : 7.5	Na ₂ SiO ₃ + NaOH	-H ₂ O ₂ : FA	- H ₂ O ₂ : 0.5 and 1.5% - SDS: 0.1- 4.0%	70°C RT	24h 3d	rho: 580–1340 kg/m ³	[44]

	CaO: 6.1 MgO: 2.5 K ₂ O: 2.2 Na ₂ O: 0.8		-sodium dodecyl sulfate SDS : SA				CS: 2.6–12.2 MPa EOC FS: 2.9–3.9 EOC	
	SiO ₂ : 38.3 Al ₂ O ₃ : 52.2 Fe ₂ O ₃ : 1.9 CaO: 1.1 MgO: <0.1 K ₂ O: 0, 4 Na ₂ O: <0.1 TiO ₂ : 2,2 P ₂ O ₅ : 0.2 MnO: <0.1 LOI: 3.3	Na ₂ SiO ₃ + NaOH	-Oleic acid: CFA -H ₂ O ₂ : FA	-Activator/fly ash: 0.97 - Oleic acid/fly ash: 7.0% - H ₂ O ₂ /fly ash: 4.5%	80°C	10h, a	adsorption of methylene blue trihydrate: 50.7 ± 0.7 mg/g	[45]

		Na ₂ SiO ₃ + NaOH	Gas FA: silica fume, FeSi or SiC		80°C	12h, a	Rho: 540 kg/m ³ CS :2.1 MPa in 28d -temperature resistance: up to 1000°C	[46]
	SiO ₂ : 41.96 Al ₂ O ₃ : 24.01 Fe ₂ O ₃ : 10.4 CaO: 5.78 MgO :3.8 SO ₃ : 2.68 K ₂ O: 1.5 Na ₂ O: 1.05 TiO ₂ : 2.04 Others: 1.28	NaOH	-sheet glass powder as fluxing agent - SDBS (sodium dodecyl benzene sulfonate) and glutin: FA	-NaOH :10% -sheet glass powder: ~8% - FA:13%	1050 °C	2 h, a	water absorption: 126.5%, rho: 0.414 g/cm ³ CS: 6.76 MPa	[47]

	SiO ₂ : 47.83 Al ₂ O ₃ : 28.49 Fe ₂ O ₃ : 11.38 CaO: 5.51 MgO: 1.43 SO ₃ : 0.24 K ₂ O: 0.46 P ₂ O ₅ : 0.62 Na ₂ O: 0.34 TiO ₂ : 2.04 LOI: 1.82	Na ₂ SiO ₃ + NaOH		-SiO ₂ /AlO ₃ : 1.8 -Na ₂ O/SiO ₂ : 0.8 -Na ₂ O/Al ₂ O ₃ : 1.5 -H ₂ O/Na ₂ O: 12 -H ₂ O/Al ₂ O ₃ : 18 -L/S: 0.25	40°C	n.d	CS: 57 MPa in 14d	[48]
		Red mud		-red mud: 0% -60% -L/S: 0.34-0.56	23°C 60°C	1 d 3 d, a	CS (60% of red mud): 1.6 MPa	[49]
		High calcium wood ash (HCWA)		-HCWA: 50-60% to replace fly ash			Different CS and absorbance potential values	[50]
		CaO, NaOH, MgO		-L/S: 0.4	23°C	7 d	CS: 35 MPa in 28d	[51]

					RH% : 100			
		Ca(OH) ₂ + Na ₂ SiO ₃	-PVA fibers	-L/S: 0.2 -Na ₂ SiO ₃ /NaOH: 2.5 -Activating solution: 0.35	23°C	UT		[52]
	SiO ₂ : 49.9 Al ₂ O ₃ : 24.8 Fe ₂ O ₃ : 16.6 CaO: 1.79 MgO: 1.31 K ₂ O: 0.61 Na ₂ O: 0.4 TiO ₂ : 1.36 P ₂ O ₅ : 1.52 SrO: 0.33 BaO: 0.45	Bayer liquor		-Si/Al: 2.3 -Na/Al: 0.8 -H/Si: 5.5	-70°C -RT	24 h 28 d, a	CS: 43 MPa	[53]

	Others: 0.7							
		NaOH+ NaAlO ₂ + Al ₂ O ₃		-SiO ₂ /AlO ₃ : 0.75 -Na ₂ O/Al ₂ O ₃ : 1 -H ₂ O/Na ₂ O: 12 -L/S: 0.338	40°C		CS: 55 MPa in 28 d	[54]
	SiO ₂ : 42.09 Al ₂ O ₃ : 25.13 Fe ₂ O ₃ : 13.16 MnO: 0.18 CaO: 13.56 MgO: 1.27 K ₂ O: 0.41 Na ₂ O: 0.81 SO ₃ : 0.41 TiO ₂ : 1.44 P ₂ O ₅ : 1.1	Na ₂ SiO ₃ + NaOH	-Al: BA		RT 65°C	4h 6d, a	CS: 1.59-0.42 MPa Porosity: 55.6%- 66.3% rho: 800-350 kg/m ³	[55]

	SiO ₂ : 51.9 Al ₂ O ₃ : 32.8 Fe ₂ O ₃ : 6.3 CaO: 2.7 K ₂ O :2.12 TiO ₂ : 1.89	Na ₂ SiO ₃ + NaOH	-Al: BA	L/S: 0.37-0.39	22 °C 80 °C	2h 12h, a	CS: 6MPa FS :1 MPa Thermal conductivity: 0.145 (W/m/K) Thermal capacity Cp: 1089 (J/kg/K)	[56]
	SiO ₂ : 54.4 Al ₂ O ₃ : 30.6 Fe ₂ O ₃ : 3.2 CaO: 4.5 MgO: 1.1 K ₂ O: 0.8 TiO ₂ : 1.6 LOI: 0.8 Other: 0.6	NaOH	-NaOCl: FA	NaOH/fly ash: 0.2	RT 90 °C	1d 3d, a	Porosity: 35–62%. CS: 1 ± 18% MPa Mesoporous surface: 10.2.m ² /g Mesopore radius:1.9nm	[57]

	SiO ₂ : 52.5 Al ₂ O ₃ : 23.3 Fe ₂ O ₃ : 7.46 CaO: 6.09 MgO: 2.48 K ₂ O: 2.23 Na ₂ O: 0.8	Na ₂ SiO ₃ + NaOH	-Al, H ₂ O ₂ : BA		70 °C	24h, a	Porosity: 59% (Al) 48% (H ₂ O ₂) CS: 2.9-9.3 MPa Rho: 610-1000	[58]
			-Al: BA -sika lightcrete: SA and TA		70 °C	24h, a	Rho: 720-1320 kg/m ³ CS: 1.6-7.2 MPa	[59]
		Na: The alkali ion	-Al, SF, SiC, FeSi: BA -Portland cement, Lime: SA and TA		80 °C	12 h, a	Bulk density: 0.5-1 g/cm ³	[46]

	SiO ₂ : 46.77 Al ₂ O ₃ : 25.22 Fe ₂ O ₃ : 6.68 CaO: 11.15 MgO: 1.37 K ₂ O: 1.48 Na ₂ O: 1.57 TiO ₂ : 1.58 SO ₃ : 3	Na ₂ SiO ₃	H ₂ O ₂ : BA		RT 50 °C RT	24 h 10 h 7 d	Bulk density: 0.5-1.6 g/cm ³	[60]
		NaOH+ Na ₂ SiO ₃	SiC: BA		RT	30 d		[61]
	SiO ₂ : 58.83 Al ₂ O ₃ : 19.24 Fe ₂ O ₃ : 6.66 CaO: 5.51 MgO: 1.43 SO ₃ : 0.03 K ₂ O: 0.16		Al: BA		60-90°C	24h	rho: 1660-700 kg/m ³ Water absorption: 3-26% Bulk density: 0.7-1 g/cm ³	[62]

	<p>P₂O₅: 0.62</p> <p>Na₂O: 0.36</p> <p>TiO₂: 2.04</p> <p>LOI: 1.04</p> <p>Others: 2.28</p>							
			NaOCl: BA		<p>30 °C</p> <p>90 °C</p>	<p>-</p> <p>4d</p>	<p>Bulk density : 0.8</p> <p>g/cm³</p>	[57]
		Na ₂ SiO ₃ + NaOH	Al: BA	Activator/ precursor: 0.25, 0.30, 0.3.	<p>RT</p> <p>60 °C</p>	<p>24 h,</p> <p>24 h, a</p>	<p>Bulk density : 0.4-</p> <p>1.3 g/cm³</p> <p>CS: 4.35-0.9 MPa</p>	[63]
		Na ₂ SiO ₃	PVA fibers	L/S: 0.35	23 °C	UT	<p>CS: 48.7 MPa in</p> <p>28d</p>	[64]
Fly ash +glass powder		-Cleaning solution from aluminum industry			<p>85 °C</p> <p>RH> 90%</p>	20h	<p>CS :9-10 MPa in</p> <p>28d</p> <p>FS : 2.5-3 MPa</p>	[65]

		-Alkaline solution: 5M						
Fly ash +Blast furnace slag		Sugar cane Straw ash (SCSA)		-H ₂ O/ NaOH/ SCSA: 202.5/32/x where x=29.5, 44.3, 59 and 73.8	25 °C 65°C	3-7-28-90 d 3days	Different values of CS	[66]
Fly ash + metakaolin+ water treatment sludge (WTS)		NaOH			90°C ± 5°C	30 min, a	CS: 6 MPa-44 MPa in 28 d	[67]
Slag +clay		Na ₂ SiO ₃ + NaOH	A foaming agent	Na ₂ O: 4% in total weight of slag and clay	20°C RH: 95%	UT	Rho: 453-1100 Kg/m ³ CS: 3.3-14 MPa FS: 0.8-1 MPa	[68]

							Thermal conductivity of 0.116 W/(m•K)	
slag	SiO ₂ : 36.78 CaO: 35.86 Al ₂ O ₃ : 9.79 MgO: 8.94 TiO ₂ : 3.44 MnO: 0.92 FeO: 0.73 S: 1.09	Na ₂ SiO ₃ + NaOH	Al powder: BA		25-70- 87-25 °C	14 h	Rho: 200-1100 kg/m ³ CS: 1-15.3 MPa	[69]
FA+slag		Na ₂ SiO ₃ + NaOH	FA		40 °C RT	24 h 27 d	Rho: 720-1600 kg/m ³ CS: 3-48 MPa in 28d The thermal conductivity: 0.15-0.48 W/m·K	[70]

FA		Na ₂ SiO ₃ + NaOH	Al powder: BA		60°C	24h after unmould ing	Rho: 403-1309 kg/m ³ CS: 0.9-4.35 MPa	[63]
Rice husk (R) and volcanic (P) ashes		NaOH	Al powder: BA				Thermal conductivity [W/(m.K)] :0.15 - 0.4	[71]
FA+slag		-Ca(OH) ₂ Mg(NO ₃) ₂ -Ca(OH) ₂ Na ₂ SiO ₃ -Ca(OH) ₂ Na ₂ SiO ₃	Pre-foaming Surfactant: protein with enzymatic active components		RT	UT	Rho: 325 – 492 kg/m ³ CS : 0.5 - 1.97 MPa	[72]
MK - Glass waste - stellplant waste		Na ₂ SiO ₃	aluminium nitride		80 °C	24h	Rho: 380 – 470 kg/m ³ CS: 1.1- 2.0 MPa	[73]

							Thermal conductivity [W/(m.K)] :0.14 - 0.15	
Volcanic glass (perlite)	SiO ₂ :71.58 Al ₂ O ₃ : 13.23 K ₂ O: 4.02 Na ₂ O: 3.36 CaO: 2.12 Fe ₂ O ₃ : 1.83 MgO: 1.04 H ₂ O: 2.5	NaOH	H ₂ O ₂ : BA		35 °C	24h	Rho: 300-665 kg/m ³ CS :0.25-0.78MPa	[74]
Fly ash +Palm oil fuel ash		NaOH + Na ₂ SiO ₃		- Palm oil fuel ash: 20% - Fly ash: 80% NaOH/Na ₂ SiO ₃ : 2.5	65 °C	48	Rho: 1300–1700 kg/m ³ CS: 8.32–30.1 MPa FS: 1.48–3.76 MPa	[75]

Natural Soil	SiO ₂ : 62.81 Al ₂ O ₃ : 22.37 Fe(OH) ₃ : 11.47 TiO ₂ : 1.11	NaOH + Na ₂ SiO ₃	H ₂ O ₂ : BA	- H ₂ O ₂ :33% -NaOH: 6-8% -Na ₂ SiO ₃ : 14-20%	60 °C 220 °C	24 24-28 h	Rho: 861–1090 kg/m ³ CS : 2.41–1.57 MPa	[76]
MK+(Epoxy resin or dimethylsiloxane)		NaOH + Na ₂ SiO ₃	Si powder: FA	Si powder: 0.03 and 0.24%	22 °C 60 °C	0–24 24-48	Rho: 250–850 kg/m ³ CS: 0.1–11MPa	[77]
Calcined ore-dressing tailing of bauxite + blast furnace slag		NaOH + Na ₂ SiO ₃		-Calcined tailing: 70% -Slag: 30%	RT	6 years	CS: 75.0 MPa in 6th years	[78]
Granulated blast slag with high MgO content		Anhydrous Na ₂ CO ₃ and Na ₂ SiO ₃		MgO: 16.1%	20 °C	28 d		[79]

FA+mk+waste sandstone sludge		NaOH 8 M and 12 M			85 °C	5 or 20 h	Mechanical strength 36 MPa	[80]
Electric arc furnace slag +red mud+other industrial waste		NaOH + Na ₂ SiO ₃		L/S: 0.27 and 0.33	80 °C	24h		[81]
Waste glass (fluorescent lamps) + MK		NaOH + Na ₂ SiO ₃		Waste glass: 37.5%	40 °C RT	1d 27d	CS: 14 MPa in 28 d	[82]
Slag, municipal solid waste incineration bottom ash and waste granite powder		NaOH + Na ₂ SiO ₃			RT		CS: 20-70 MPa	[83]

Marble, travertine and vulcanic tuff wastes		NaOH			22 °C	90 d		[84]
--	--	------	--	--	-------	------	--	------

LOI: loss on ignition at 1000°C

EOC: end of curing

a: cured at ambient conditions afterwards until testing

RT: room temperature

CS: compressive strength

FS: flexural strength

d: day

h: hour

rho: volumetric mass

CFA: chemical foaming agent

BA: blowing agent

SA: stabilizing agents




TA: thickening agents



T°: temperature





RH: relative humidity




PVA: polyvinyl alcohol




Table A2 : resulting geopolymers' description





Sample	State	Color	Strength	Image
1	Liquid	Light grey	-	
	Solid	White	Fragile and easily powdered	
2	Solid	White	Fragile and easily powdered	-
3	Viscous liquid	Dark grey	-	





	Solid	Grey	Easily breakable	-
4	Plasticine aspect with bubbles inside	Dark Grey	-	
	Two phases, both have a viscous liquid aspect	Darker grey – black	-	-
5	The sample in the full mold has the shape of Plasticine with bubbles inside	Dark grey	-	

	The sample in the half-full mold is solid	Grey	Easily breakable	
6	Plasticine aspect	Dark grey	-	
	Hard solid layer on the top and viscous liquid inside	Grey	-	
7	Plasticine aspect	Dark grey	-	


	Hard solid layer on the top and viscous liquid inside	Grey	-	
8	Plasticine aspect	Dark grey	-	
	Hard solid layer on the top and viscous liquid inside	Grey	-	

9	Viscous liquid	Grey	-	-
	Two phases, both have a viscous liquid aspect	Grey-black	-	
10	Two phases, both have a viscous liquid aspect	Grey-black	-	
11	Hard solid layer on the top and viscous liquid inside	Grey-black	-	-
12	Two phases, both have a viscous liquid aspect	Orange	-	

13	Two phases, both have a viscous liquid aspect	Grey-black	-	
14	Solid	Grey	Susceptible to being broken by hands	
15	Solid	Grey	Susceptible to being broken by hands	
16	Viscous liquid covered by a solid layer	Black	-	

17	Viscous liquid covered by a bright layer	Black	-	
18	Viscous liquid covered by a bright layer	Black	-	
19	Viscous liquid covered by a bright layer	Black	-	
20	Viscous liquid covered by a bright layer	Black	-	-
21	Solid grains	Grey	-	

22	Solid grains	Grey	-	
23	Solid	Dark grey	-	
24	Solid	Light grey	-	

25	Solid	Dark grey	-	
26	Solid	Light grey	-	